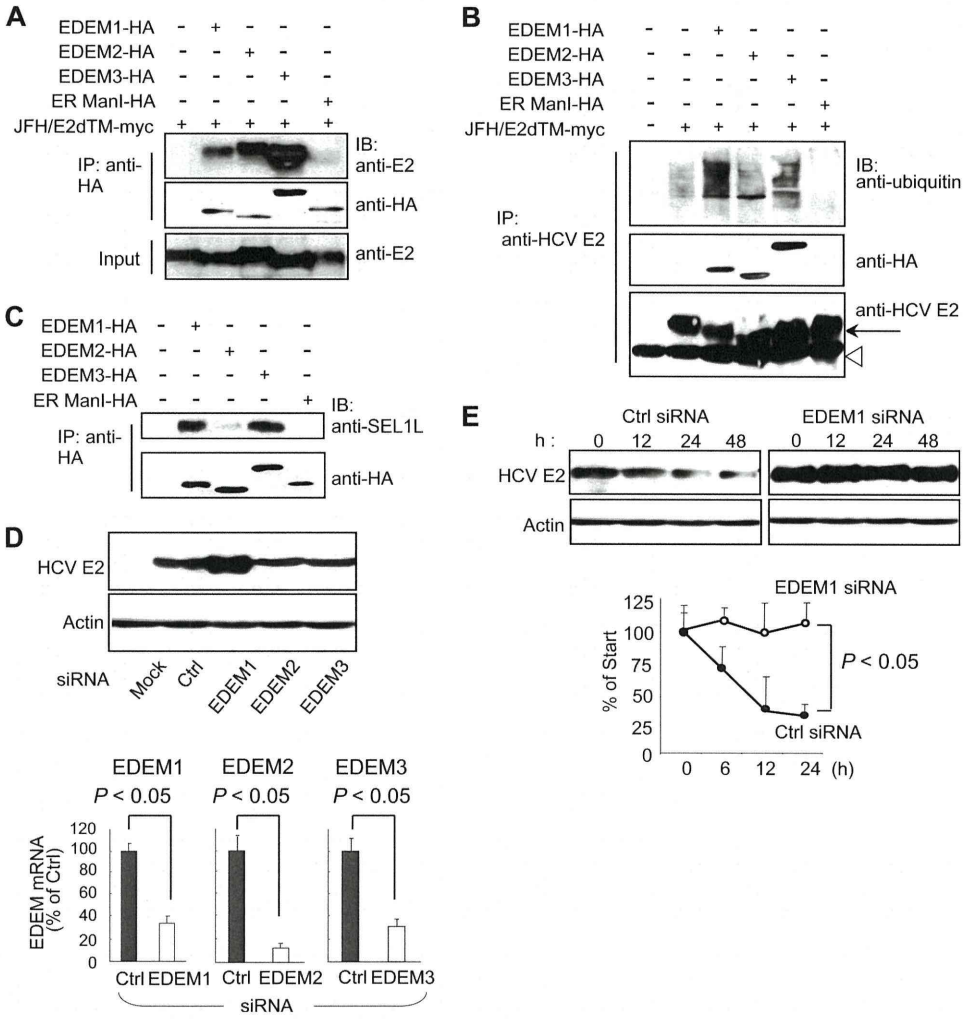

FIGURE 3. **EDEMs are involved in the degradation of HCV glycoproteins.** *A*, binding of EDEMs and ER ManI with HCV E2. 293T cells were seeded in 6-well plates at a density of 3×10^5 cells/well. After overnight incubation, cells were co-transfected with plasmids carrying HCV E2-myc (1 μg) and EDEM1-HA, EDEM2-HA, EDEM3-HA, or ER ManI-HA proteins (1 μg each). Forty-eight hours later, cells were harvested, immunoprecipitated (*IP*) with anti-HA antibodies, and Western blotting (*IB*) was performed with the indicated antibodies. *B*, ubiquitylation of HCV E2 protein in cells co-transfected with HCV E2 and EDEM plasmids. 293T cells were seeded in 6-well plates at a density of 3×10^5 cells/well. Twenty-four hours later, the cells were co-transfected with plasmids carrying HCV E2-myc (1 μg) and EDEM1-HA, EDEM2-HA, EDEM3-HA, or ER ManI-HA genes (1 μg each). Forty-eight hours later, the cells were harvested and immunoprecipitated with anti-E2 antibodies, and Western blotting was performed with the indicated antibodies. *Arrow*, HCV E2; *open arrowhead*, immunoglobulin heavy chain. *C*, binding of EDEMs and ER ManI with endogenous SEL1L in cells. *D*, steady-state level of HCV E2 in HCV-infected HuH-7 cells after EDEM knockdown (*upper*). The knockdown efficiencies of the respective siRNAs are shown in the *lower panel*. Values are normalized to GAPDH expression levels, and normalized values in negative control cells have been arbitrarily set at 100%. *E*, stability of HCV E2 protein in EDEM1 knockdown cells. HCV-infected HuH-7 cells were transfected with control or EDEM1 siRNA. Forty hours later, the cells were exposed to CHX (100 μg/ml) for 0, 12, 24, and 48 h, followed by immunoblotting. Specific signals were quantified by densitometry, and the percent of HCV E2 remaining was compared with initial levels. The mean ± S.D. (*error bars*) of two independent experiments are shown.

on virus production was observed following EDEM2 gene silencing (Fig. 4*A*). On the other hand, no significant differences were observed with regard to intracellular HCV core protein levels among mock- and EDEM siRNA-transfected cells (Fig. 4*B*), which indicates that replication of the viral genome is not affected by EDEM proteins. To examine further whether this effect on virus production was due to turnover of HCV envelope proteins, we performed loss-of-EDEM-function experiments in HuH-7 cells carrying HCV subgenomic replicons. Because the replicons do not require envelope proteins, they should be insensitive to the expression levels of genes involved in the ERAD pathway. As expected, siRNA-mediated knockdown of EDEMs resulted in little to no change in genome replication (supplemental Fig. S4*A*). To investigate further the participation of EDEMs in the HCV life cycle, HCV-infected cells were examined 48 h after transfection with an expression plasmid for either EDEM1, EDEM2, or EDEM3. As expected, exogenous expression of EDEM1 in the infected cells led to a 2.4-fold decrease in virus production compared with mock-transfected cells ($p < 0.05$) (Fig. 4*C*). A moderate decrease of 1.7-fold was observed in the cells overexpressing EDEM3 protein. Ectopic expression of EDEMs and ER ManI did not cause any change in intracellular HCV core protein levels (Fig. 4*D*). Similarly, little or no change was observed in genome replication when plasmids carrying EDEMs were introduced into HCV subgenomic replicon cells (supplemental Fig. S4*B*). These results indicate that EDEM1 and EDEM3, particularly EDEM1, regulate virus production, possibly through post-translational control of HCV glycoproteins.

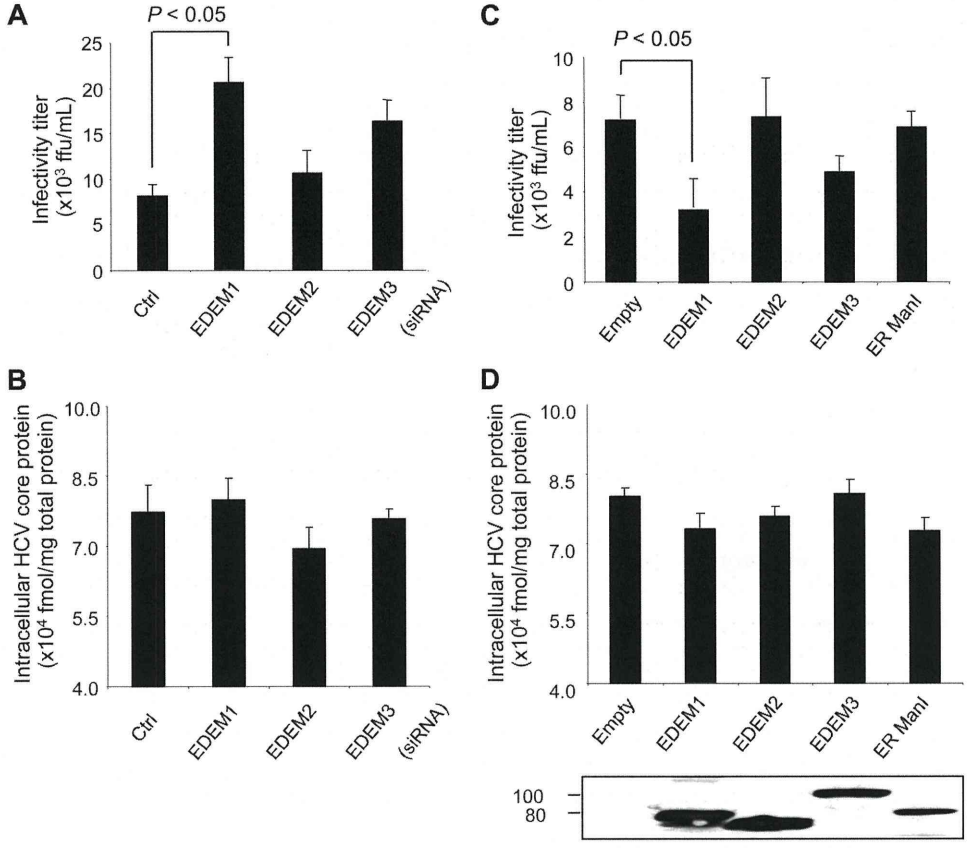

FIGURE 4. **Role of EDEMs in HCV replication and production of infectious virus particles.** *A*, HCV production in HuH-7 cells transfected with EDEM siRNAs. Cells were infected with JFH-1 at a m.o.i. of 1. Twenty-four hours later, the cells were transfected with the indicated siRNAs at a final concentration of 10 nM. The culture medium was harvested 48 h later and was used to infect naïve HuH-7.5.1 cells seeded in a 96-well plate. Immunostaining using anti-HCV core antibodies was performed at 72 h after infection, and focus-forming units were counted. *B*, siRNA-transfected and HCV-infected cells described in *A* harvested at 48 h after infection. Intracellular HCV core protein was measured. The values were normalized to total protein in the cell lysate samples. *C*, HCV production in HuH-7 cells transfected with plasmids carrying EDEM1-HA, EDEM2-HA, EDEM3-HA, or ER ManI-HA genes. *D*, intracellular HCV core protein within the cells described in *C*. Expression levels of the EDEMs and ER ManI were determined by anti-HA immunoblotting. The mean ± S.D. (*error bars*) of three independent experiments are shown in all of the *panels*.

Chemical Inhibition of the ERAD Pathway Increases HCV Production—KIF, a potent inhibitor of ER mannosidase, is reported to inhibit the ERAD pathway. When HCV-infected cells were treated with KIF, virus production increased in the culture medium in a dose-dependent manner (Fig. 5*A*, *left*), and the steady-state level of E2 in the cells increased accordingly (Fig. 5*A*, *right*). No change was observed in intracellular HCV core protein levels after KIF treatment (Fig. 5*A*, *center*). Kinetic analyses showed that E2 was stabilized dramatically in KIF-treated cells (Fig. 5*B*), whereas the fate of HCV core protein, a nonglycoprotein, was not affected by KIF treatment (supplemental Fig. S5). No effect on virus replication was observed when the cells harboring JFH-1 subgenomic replicons were treated with KIF (data not shown).

On the basis of these findings, one may hypothesize that KIF contributes to the stabilization of HCV glycoprotein(s) by interfering with the interaction between (i) EDEMs and viral proteins, or (ii) EDEMs and SEL1L. To address this, HCV E2 was co-expressed in 293T cells with EDEM1, EDEM2, EDEM3, or ER ManI in the presence or absence of KIF, followed by immunoprecipitation (Fig. 5*C*). E2 was shown to interact with EDEM1, EDEM2, and EDEM3, analogous to the data shown in Fig. 3*A*, and KIF did not block the interactions. Decreased electrophoretic mobility of E2 was detected in KIF-treated cells, possibly due to a change in glycan composition caused by inhibition of mannosidase activity. These findings led us to investigate whether the glycans on HCV glycoproteins are required for binding to EDEMs. We generated E1 and E2 mutants by replacing their *N*-glycosylation sites with glutamine residues and analyzed their interaction with EDEMs. Removal of the glycans did not inhibit the binding of E1 and E2 proteins to EDEM, demonstrating that *N*-glycans on the surface of viral proteins are not indispensible for an interaction between EDEMs and HCV glycoproteins to occur (supplemental Fig. S6). The effect of KIF on the association of EDEMs with downstream ERAD machinery was examined further. In cells co-expressing E2 and EDEMs, the interaction of SEL1L with EDEM1 and EDEM3 was significantly reduced in the presence of KIF ($p < 0.05$) (Fig. 5*C*). Consistent with these results, KIF abrogated the EDEM1- and EDEM3-mediated ubiquitylation of HCV E2 protein (Fig. 5*D*). This inhibitory effect of KIF on the SEL1L-EDEM interaction was also observed in HuH-7 cells (supplemental Fig. S7). These results suggest that KIF stabilizes HCV glycoproteins by interfering with the SEL1L-EDEM interaction and thus leads to an increase in virus production.

Role of ERAD in the Life Cycle of JEV—This study demonstrates involvement of the ERAD pathway in HCV production. However, the role of this pathway in the production of other

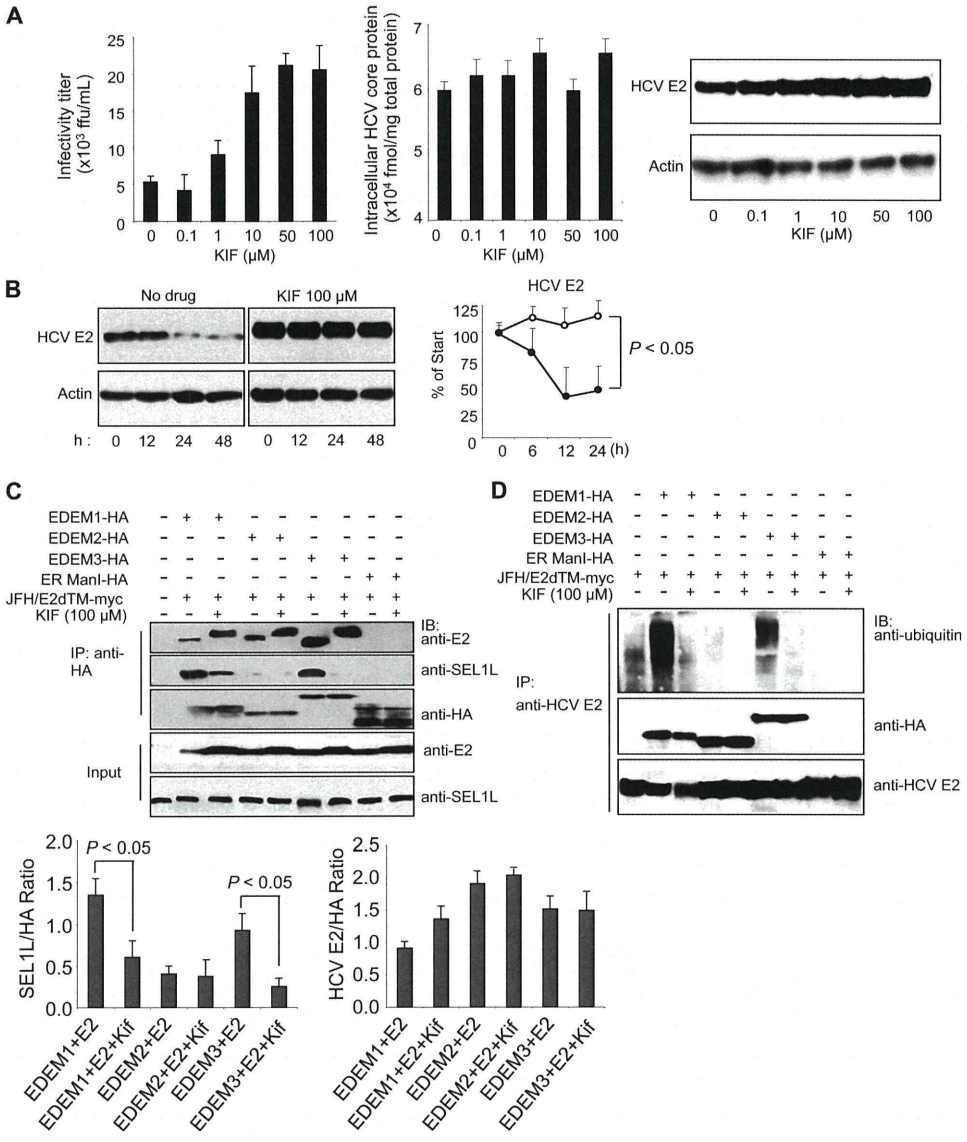

FIGURE 5. **Effect of KIF on HCV production and stability of E2.** *A*, extracellular HCV titer, intracellular HCV core protein expression, and steady-state level of HCV E2 in HuH-7 cells treated with different concentrations of KIF. *B*, CHX-based HCV protein stability assay of HCV E2 protein in KIF-treated cells as described in Fig. 3*E*. E2 protein levels normalized to actin levels are shown in the *graph* on the *right*. The *open* and *filled circles* indicate KIF-treated and nontreated cells, respectively. The mean ± S.D. (*error bars*) of two independent experiments are shown. *C*, binding of EDEMs and ER ManI with HCV E2 and SEL1L in 293T cells in the absence or presence of KIF. 293T cells were seeded in 6-well plates at a density of 3×10^5 cells/well. After overnight incubation, the cells were co-transfected with plasmids carrying HCV E2-myc (1 μg) and EDEM1-HA, EDEM2-HA, EDEM3-HA, or ER ManI-HA proteins (1 μg each). After 6 h, the culture medium was replaced with fresh or KIF-containing medium (100 μM). Forty-eight hours later, the cells were harvested and immunoprecipitated (*IP*) with anti-HA antibodies, after which Western blotting (*IB*) was performed with the indicated antibodies. Specific signals were quantified by densitometry, and the ratio between HCV E2 and HA (*right graph*) and between SEL1L and HA (*left graph*) in the same *lanes* is plotted on the graphs. The mean ± S.D. of three independent experiments are shown. *D*, EDEM protein-mediated ubiquitylation of HCV E2 protein in 293T cells in the absence or presence of KIF. The experimental procedure was the same as that described in Fig. 5*C*, except that immunoprecipitation was performed with anti-HCV E2 antibodies.

viruses is still unknown. To this end, we examined its role in the life cycle of JEV, another member of the Flaviviridae family. In contrast to HCV, KIF treatment had little effect on JEV production in infected cells (Fig. 6*A*) or the steady-state level of viral E glycoprotein (Fig. 6*B*). Interaction of EDEMs with JEV E was analyzed further. Neither EDEMs nor ER ManI was found to interact with JEV E in cells (Fig. 6*C*), indicating no significant role of the ERAD pathway in the JEV life cycle. Altogether, these results strongly suggest that the ERAD pathway is involved in the quality control of glycoproteins of specific viruses, possible through an interaction with EDEM(s), and subsequent regulation of virus production.

DISCUSSION

Accumulating evidence points to a role of the ERAD pathway in the pathogenesis of different genetic and degenerative diseases. However, the involvement of ERAD in the life cycle of viruses and infectious diseases remains poorly understood. Until recently, an experimental HCV cell culture infection system has been lacking such that studies evaluating the effect of HCV infection on the ERAD pathway were performed by either using HCV subgenomic replicons which lack structural proteins or by ectopic expression of one or multiple structural proteins (21, 22). However, this problem was solved by identifica-

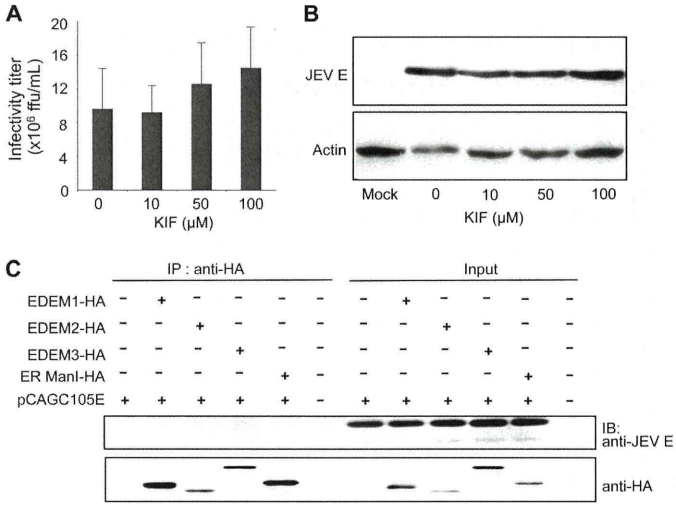

FIGURE 6. **Binding of JEV envelope glycoprotein with EDEMs and effect of KIF on JEV production.** *A*, JEV production in HuH-7 cells treated with KIF. The mean ± S.D. (*error bars*) of three independent experiments are shown. *B*, effect of KIF on the steady-state level of JEV envelope protein. *C*, binding of EDEMs with the JEV envelope.

tion of an HCV clone, JFH-1, capable of replicating and assembling infectious virus particles in cultured hepatocytes (15). In the present study, we used JFH-1 to examine the effect of HCV infection on activation of the ERAD pathway and its role in the virus life cycle. Our results show that the ERAD pathway is activated in HCV-infected cells, as evidenced by the maturation of XBP1 mRNA to its active form and up-regulation of EDEM1 (Fig. 1, *A–D*). Knocking down IRE1 reversed the induction of EDEM1, indicating that HCV infection-induced activation of the ERAD pathway is mediated through IRE1 (Fig. 1*F*). Loss- and gain-of-function analyses indicated that EDEM1 and EDEM3, particularly EDEM1, are involved in the post-translational control of HCV glycoproteins by which viral production is down-regulated (Figs. 3, *D* and *E*, and 4*A*). Our results suggest that EDEM1 and EDEM3 play a role in delivery of viral glycoproteins to the SEL1L-containing ubiquitin-ligase complex. It has recently been reported that coronavirus infection causes an accumulation of EDEM1 in membrane vesicles which are sites of viral replication, but that EDEM1 is not required for coronavirus replication (23). To our knowledge, the present study is the first to demonstrate regulation of the viral life cycle by ERAD machinery through interaction of EDEMs with viral glycoproteins.

We propose that the mechanisms described here are important during the early stages of establishing persistent HCV infection. ER stress caused by high levels of HCV infection during the acute phase presumably results in activation of the ERAD pathway. Induced EDEMs enhance the degradation of HCV envelope proteins, thereby reducing virus production. Maintenance of moderately low levels of HCV in the infected liver may contribute to the persistence of HCV infection, often associated with a lengthy asymptomatic phase that can last for decades. A range of viruses, including flaviviruses such as JEV, dengue virus, and West Nile virus, have been reported to induce XBP1 mRNA splicing triggered by ER stress (2, 3, 24). However, we demonstrate here that, in contrast to HCV, the envelope protein of JEV, which causes acute encephalitis, is not recognized by EDEMs, and the ERAD pathway does not control JEV production.

N-Linked glycoproteins displaying the glycan precursor Glc1Man9GlcNAc2 bind ER chaperones, such as calnexin or calreticulin, which facilitates protein folding. Removal of the terminal Glc from glycans disrupts this interaction with chaperones leading to Man trimming and delivery to ERAD machinery. A glucosyltransferase can transfer the terminal Man-linked Glc back to glycans, thereby allowing the "calnexin cycle" to continue until the glycoproteins are properly folded (for review, see Ref. 25). During this cycle, the decision of when to abandon additional folding attempts for immature polypeptides and to direct them instead toward the degradation pathway appears to be a crucial element of protein quality control. The basis by which this occurs, however, is not fully understood. Here, we demonstrate that stabilization of HCV envelope proteins and increased virus production occurs with KIF treatment (Fig. 5, *A* and *B*) and with gene silencing of either EDEM1 or EDEM3 (Figs. 3, *D* and *E*, and 4*A*). It is generally accepted that ERAD functions to eliminate proteins that are unable to adopt their native structure after translocation into the ER. From our results, however, one could argue that, during the HCV life cycle, at least a fraction of the competently folded viral glycoprotein intermediates may be released from the calnexin cycle before maturation and thereby be recognized as ERAD substrates. As suggested previously, the processes of protein folding and ERAD compete to some extent for newly synthesized polypeptides (26, 27). Under conditions in which high concentrations of ERAD-related factors are found in the ER due to induction of ER stress by viral infection, activated ERAD machinery may efficiently capture protein intermediates with folding/refolding capacity and cause premature termination of chaperone-assisted protein folding.

EDEM1 has recently been found to bind SEL1L, which is involved in the translocation of ERAD substrates from the ER to the cytoplasm (20). Our results demonstrate efficient binding of EDEM1 and EDEM3 to SEL1L, whereas EDEM2 exhibits only residual binding. In agreement with these results, increased ubiquitylation of HCV E2 protein was observed in cells overexpressing EDEM1 and EDEM3, but not in cells overexpressing the EDEM2 ortholog (Fig. 3*B*). Furthermore, KIF inhibited the binding of EDEM1 and EDEM3 with SEL1L, thus abrogating the ubiquitylation and enhancing the stability of HCV E2 protein (Fig. 5, *B* and *D*). It has been reported that KIF inhibits the interaction between EDEM1 and SEL1L, thus stabilizing ERAD substrates (4). Therefore, our results confirm previous findings and show that, along with EDEM1, KIF inhibits the binding of SEL1L to EDEM3. Furthermore, we have been the first to show that HCV E2 is a virus-derived ERAD substrate that can be used to analyze the mechanisms of this pathway. Taken together, our results indicate that EDEM1 and EDEM3, but not EDEM2, might be involved in targeting ERAD substrates to the translocation machinery, which may partly explain the different roles of the three EDEMs in HCV production. Although both EDEM1 and EDEM3 bind SEL1L and HCV envelope proteins, EDEM1 appears to have a larger role in regulation of HCV production than EDEM3. This is supported further by the finding that enhanced ubiquitylation of HCV E2 occurs in the presence

of EDEM1 overexpression (Figs. 3*B* and 5*D*). In EDEM3-knockdown cells, EDEM1 may take over the function of delivering ERAD substrates to the translocation machinery. We also speculate that EDEM1 may function as a helper for EDEM3. This is supported by the observation that EDEM1 and EDEM3 synergistically increase HCV production when knocked down together (data not shown). HCV glycoproteins are a suitable means by which to investigate differences and redundancies pertaining to the role of EDEMs in the ERAD pathway.

HCV-infected and TM-treated cells demonstrated the greatest activation of EDEM1 transcript production among EDEMs (Fig. 1, *C* and *D*, and supplemental Fig. S1). Although it is known that XBP1 binds to specific ER stress-responsive *cis*-acting elements to induce EDEMs (28, 29), the exact mechanism of transcriptional regulation is not fully understood. It will be interesting to examine regulatory mechanism(s) specific to individual EDEM homologs in an ER stress-dependent or -independent manner.

These findings highlight the crucial role of the ERAD pathway in the HCV life cycle. Further studies are needed to clarify the details of this complex pathway. The data generated in this work, however, further contribute to our understanding of the mechanisms that govern the maturation and fate of viral glycoproteins in the ER.

Acknowledgments—We thank Dr. F. V. Chisari for the HuH-7.5.1 cells, Drs. N. Hosokawa and K. Nagata for the EDEM expression plasmids, Dr. K. Mori for the reporter plasmids of GRP78 and GRP94, and Drs. C. K. Lim and T. Takasaki for the anti-JEV antibody. We thank Drs. Chia-Yi Yu and Yi-Ling Lin for valuable advice and T. Date, M. Kaga, M. Sasaki, and T. Mizoguchi for assistance.

REFERENCES

1. Vembar, S. S., and Brodsky, J. L. (2008) *Nat. Rev. Mol. Cell Biol.* **9,** 944–957
2. Yu, C. Y., Hsu, Y. W., Liao, C. L., and Lin, Y. L. (2006) *J. Virol.* **80,** 11868–11880
3. Barry, G., Fragkoudis, R., Ferguson, M. C., Lulla, A., Merits, A., Kohl, A., and Fazakerley, J. K. (2010) *J. Virol.* **84,** 7369–7377
4. Isler, J. A., Skalet, A. H., and Alwine, J. C. (2005) *J. Virol.* **79,** 6890–6899
5. Helenius, A., and Aebi, M. (2004) *Annu. Rev. Biochem.* **73,** 1019–1049
6. Mast, S. W., Diekman, K., Karaveg, K., Davis, A., Sifers, R. N., and Moremen, K. W. (2005) *Glycobiology* **15,** 421–436
7. Hirao, K., Natsuka, Y., Tamura, T., Wada, I., Morito, D., Natsuka, S., Romero, P., Sleno, B., Tremblay, L. O., Herscovics, A., Nagata, K., and Hosokawa, N. (2006) *J. Biol. Chem.* **281,** 9650–9658
8. Bartenschlager, R., and Lohmann, V. (2000) *J. Gen. Virol.* **81,** 1631–1648
9. Reed, K. E., and Rice, C. M. (2000) *Curr. Top. Microbiol. Immunol.* **242,** 55–84
10. Zhong, J., Gastaminza, P., Cheng, G., Kapadia, S., Kato, T., Burton, D. R., Wieland, S. F., Uprichard, S. L., Wakita, T., and Chisari, F. V. (2005) *Proc. Natl. Acad. Sci. U.S.A.* **102,** 9294–9299
11. Zhao, Z., Date, T., Li, Y., Kato, T., Miyamoto, M., Yasui, K., and Wakita, T. (2005) *J. Gen. Virol.* **86,** 2209–2220
12. Tani, H., Shiokawa, M., Kaname, Y., Kambara, H., Mori, Y., Abe, T., Moriishi, K., and Matsuura, Y. (2010) *J. Virol.* **84,** 2798–2807
13. Yoshida, H., Haze, K., Yanagi, H., Yura, T., and Mori, K. (1998) *J. Biol. Chem.* **273,** 33741–33749
14. Murakami, K., Kimura, T., Osaki, M., Ishii, K., Miyamura, T., Suzuki, T., Wakita, T., and Shoji, I. (2008) *J. Gen. Virol.* **89,** 1587–1592
15. Wakita, T., Pietschmann, T., Kato, T., Date, T., Miyamoto, M., Zhao, Z., Murthy, K., Habermann, A., Kräusslich, H. G., Mizokami, M., Bartenschlager, R., and Liang, T. J. (2005) *Nat. Med.* **11,** 791–796
16. Lim, C. K., Takasaki, T., Kotaki, A., and Kurane, I. (2008) *Virology* **374,** 60–70
17. Takeuchi, T., Katsume, A., Tanaka, T., Abe, A., Inoue, K., Tsukiyama-Kohara, K., Kawaguchi, R., Tanaka, S., and Kohara, M. (1999) *Gastroenterology* **116,** 636–642
18. Deng, L., Adachi, T., Kitayama, K., Bungyoku, Y., Kitazawa, S., Ishido, S., Shoji, I., and Hotta, H. (2008) *J. Virol.* **82,** *10375–10385*
19. Masaki, T., Suzuki, R., Saeed, M., Mori, K., Matsuda, M., Aizaki, H., Ishii, K., Maki, N., Miyamura, T., Matsuura, Y., Wakita, T., and Suzuki, T. (2010) *J. Virol.* **84,** *5824–5835*
20. Cormier, J. H., Tamura, T., Sunryd, J. C., and Hebert, D. N. (2009) *Mol. Cell* **34,** 627–633
21. Tardif, K. D., Mori, K., Kaufman, R. J., and Siddiqui, A. (2004) *J. Biol. Chem.* **279,** 17158–17164
22. Chan, S. W., and Egan, P. A. (2005) *FASEB J.* **19,** 1510–1512
23. Reggiori, F., Monastyrska, I., Verheije, M. H., Calì, T., Ulasli, M., Bianchi, S., Bernasconi, R., de Haan, C. A., and Molinari, M. (2010) *Cell Host Microbe* **7,** 500–508
24. Medigeshi, G. R., Lancaster, A. M., Hirsch, A. J., Briese, T., Lipkin, W. I., Defilippis, V., Früh, K., Mason, P. W., Nikolich-Zugich, J., and Nelson, J. A. (2007) *J. Virol.* **81,** 10849–10860
25. Molinari, M. (2007) *Nat. Chem. Biol.* **3,** 313–320
26. Eriksson, K. K., Vago, R., Calanca, V., Galli, C., Paganetti, P., and Molinari, M. (2004) *J. Biol. Chem.* **279,** 44600–44605
27. Wu, Y., Swulius, M. T., Moremen, K. W., and Sifers, R. N. (2003) *Proc. Natl. Acad. Sci. U.S.A.* **100,** 8229–8234
28. Olivari, S., Galli, C., Alanen, H., Ruddock, L., and Molinari, M. (2005) *J. Biol. Chem.* **280,** 2424–2428
29. Yoshida, H., Matsui, T., Hosokawa, N., Kaufman, R. J., Nagata, K., and Mori, K. (2003) *Dev. Cell* **4,** 265–271

Journal of General Virology (2011), **92**, 2082–2087 DOI 10.1099/vir.0.032391-0

Short Communication

Structural requirements of virion-associated cholesterol for infectivity, buoyant density and apolipoprotein association of hepatitis C virus

Mami Yamamoto,[1,2] Hideki Aizaki,[1] Masayoshi Fukasawa,[3] Tohru Teraoka,[2] Tatsuo Miyamura,[1] Takaji Wakita[1] and Tetsuro Suzuki[1,4]

Correspondence
Tetsuro Suzuki
tesuzuki@hama-med.ac.jp

[1]Department of Virology II, National Institute of Infectious Diseases, Toyama 1-23-1, Shinjuku-ku, Tokyo 162-8640, Japan

[2]United Graduate School of Agricultural Science, Tokyo University of Agriculture and Technology, Saiwai-cho 3-5-8, Fuchu, Tokyo 183-8509, Japan

[3]Department of Biochemistry and Cell Biology, National Institute of Infectious Diseases, Toyama 1-23-1, Shinjuku-ku, Tokyo 162-8640, Japan

[4]Department of Infectious Diseases, Hamamatsu University School of Medicine, Handayama 1-20-1, Higashi-ku, Hamamatsu 431-3192, Japan

Received 22 March 2011
Accepted 17 May 2011

Our earlier study has demonstrated that hepatitis C virus (HCV)-associated cholesterol plays a key role in virus infectivity. In this study, the structural requirement of sterols for infectivity, buoyant density and apolipoprotein association of HCV was investigated further. We removed cholesterol from virions with methyl β-cyclodextrin, followed by replenishment with 10 exogenous cholesterol analogues. Among the sterols tested, dihydrocholesterol and coprostanol maintained the buoyant density of HCV and its infectivity, and 7-dehydrocholesterol restored the physical appearance of HCV, but suppressed its infectivity. Other sterol variants with a 3β-hydroxyl group or with an aliphatic side chain did not restore density or infectivity. We also provide evidence that virion-associated cholesterol contributes to the interaction between HCV particles and apolipoprotein E. The molecular basis for the effects of different sterols on HCV infectivity is discussed.

Hepatitis C virus (HCV) is a major cause of liver diseases, and is an enveloped, plus-strand RNA virus of the genus *Hepacivirus* of the family *Flaviviridae*. The mature HCV virion is considered to consist of a nucleocapsid, an outer envelope composed of the viral E1 and E2 proteins and a lipid membrane. Production and infection of several enveloped viruses, such as human immunodeficiency virus type 1 (HIV-1), hepatitis B virus and varicella-zoster virus (Bremer *et al.*, 2009; Campbell *et al.*, 2001; Graham *et al.*, 2003; Hambleton *et al.*, 2007), are dependent on cholesterol associated with virions. However, except for HIV-1 (Campbell *et al.*, 2002, 2004), there is limited information about the effects of replacing cholesterol with sterol analogues on the virus life cycle. We demonstrated the higher cholesterol content of HCV particles compared with host-cell membranes, and that HCV-associated cholesterol plays a key role in virion maturation and infectivity (Aizaki *et al.*, 2008). Recently, by using mass spectrometry, Merz *et al.* (2011) identified cholesteryl esters, cholesterol, phosphatidylcholine and sphingomyelin as major lipids of purified HCV particles.

To investigate further the effect of the structural requirement for cholesterol on the infectivity, buoyant density and apolipoprotein association of HCV, depletion of virion-associated cholesterol and substitution of endogenous cholesterol with structural analogues (Fig. 1a) was used in this study. HCVcc (HCV grown in cell culture) of the JFH-1 isolate (Wakita *et al.*, 2005), prepared as described previously (Aizaki *et al.*, 2008), was treated with 1 mM methyl β-cyclodextrin (B-CD), which extracts cholesterol from biological membranes, for 1 h at 37 °C. The cholesterol-depleted virus was then incubated with exogenous cholesterol or cholesterol analogues at various concentrations for 1 h. After removal of B-CD and free sterols by centrifugation at 38 000 r.p.m. (178 000 ***g***) for 2.5 h, the treated particles were used to infect Huh7 cells, kindly provided by Dr Francis V. Chisari (The Scripps Research Institute, La Jolla, CA, USA), and their infectivity was determined by quantifying the viral core protein in cells using an enzyme immunoassay (Ortho-Clinical Diagnostics) at 3 days post-infection (p.i.). Virus infectivity, which fell to <20 % after B-CD treatment, was

A supplementary table and figure are available with the online version of this paper.

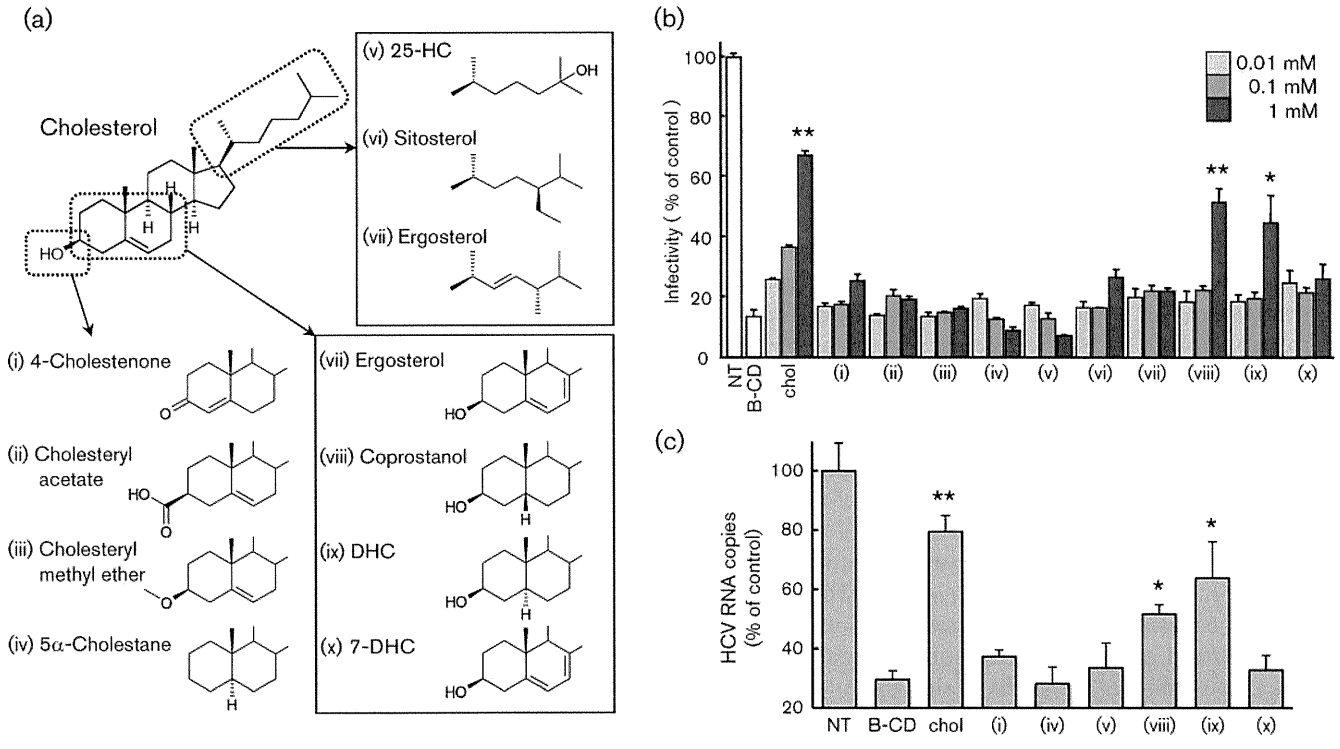

Fig. 1. Role of virion-associated cholesterol analogues in virus infection. (a) Structures of sterols used in this study. Variations in the 3β-hydroxyl group (lower left), aliphatic side chain (upper right) or ring structure (lower right) of cholesterol are shown. (i–x) Compounds studied in (b) and (c). (b) Effect of replenishment with sterols on HCV infectivity. Intracellular HCV core levels were determined at 72 h p.i. as the indicator of infectivity, which is represented as a percentage of the untreated HCVcc level (NT). (c) Effects of virion-associated sterols on virus internalization. HCV RNA copies in cells after virus internalization were quantified and are shown as percentages of the untreated HCVcc level (NT). (b, c) Means+SD of four samples are shown. *P<0.05; **P<0.01, compared with B-CD-treated virus (unpaired Student's t-test). Data are representative of at least two experiments.

recovered by addition of cholesterol at 0.01–1 mM in a dose-dependent manner (Fig. 1b). Among the cholesterol analogues tested, variants with a 3β-hydroxyl group (4-cholestenone, cholesteryl acetate, cholesteryl methyl ether and 5α-cholestane) or variants with an aliphatic side chain [25-hydroxycholesterol (25-HC), sitosterol and ergosterol] exhibited no or little effect on the recovery of infectivity of B-CD-treated HCV (Fig. 1b, lanes i–vii). In contrast, addition of variants in the structure of the sterol rings [coprostanol or dihydrocholesterol (DHC)] at 1 mM restored infectivity to around 50 % compared with non-treated virus control (Fig. 1b, lanes viii and ix). Other variants in the ring structure [7-dehydrocholesterol (7-DHC) and ergosterol, which is also a variant with an aliphatic side chain as indicated above] did not show any increase in the infectivity of B-CD-treated virus (Fig. 1b, lanes x and vii).

We demonstrated previously that HCV-associated cholesterol plays an important role in the internalization step of the virus, but not in cell attachment during virus entry (Aizaki *et al.*, 2008). The effect of virion-associated cholesterol analogues on virus attachment to cells and following internalization was determined. HCVcc, treated with B-CD with or without subsequent replenishment with sterols, was incubated with Huh7-25-CD81 cells, which stably express CD81 (Akazawa *et al.*, 2007), for 1 h at 4 °C. As an internalization assay, the incubation temperature was shifted to 37 °C post-binding procedure and maintained for 2 h. The cells were then treated with 0.25 % trypsin for 10 min at 37 °C, by which >90 % of HCV bound to the cell surface was removed (data not shown; Aizaki *et al.*, 2008). Internalized HCV was quantified by measuring the viral RNA in cell lysates by real-time RT-PCR (Takeuchi *et al.*, 1999). B-CD treatment or supplementation with sterols of B-CD-treated HCV had little or no effect on virus attachment to the cell surface (data not shown). Regarding virus internalization (Fig. 1c), treatment of HCVcc with 1 mM B-CD resulted in approximately 70 % reduction of viral RNA. The reduced level of the internalized HCV recovered markedly to approximately 80 % of the untreated HCVcc level by replenishment with 1 mM cholesterol. In agreement with the results shown in Fig. 1(b), addition of coprostanol or DHC to the B-CD-treated virus caused a significant recovery of virus internalization, suggesting that coprostanol and DHC associated with the

virion have the ability to play a role in HCV internalization into cells, in a manner comparable to cholesterol (Fig. 1c, lanes viii and ix). No or only a little recovery of virus internalization was observed by loading with other cholesterol analogues, such as 4-cholestenone, 5α-cholestane, 25-HC or 7-DHC (Fig. 1c, lanes i, iv, v and x).

To monitor the effect of cholesterol analogues on the physical characteristics of HCV, we next investigated buoyant-density profiles by using sucrose density-gradient centrifugation, in which untreated, B-CD-treated and sterol-replenished HCVcc were concentrated and layered onto continuous 10–60 % (w/v) sucrose density gradients, followed by centrifugation at 35 000 r.p.m. (151 000 ***g***) for 14 h. Fractions were collected and analysed for the core protein. Fig. 2 shows that the virus density became higher after treatment with B-CD and that cholesterol-replenished virus shifted the density of B-CD-treated HCV to the non-treated level. Consistent with the result shown in Fig. 1(b), no effect on restoration of the buoyant densities of HCV was observed using variants with modifications in either the 3β-hydroxyl group (4-cholestenone, cholesteryl acetate and 5α-cholestane) or the aliphatic side chain (25-HC and sitosterol). In contrast, variants in the sterol ring structure (coprostanol, DHC and 7-DHC) had an ability to recover the density of B-CD-treated virus to that of non-treated virus.

Incorporation efficiency of the sterols into the cholesterol-depleted HCVcc was further determined by gas chromatography with flame ionization detection (see Supplementary Table S1, available in JGV Online). Under the experimental conditions used, exogenously supplied cholesterol after B-CD treatment was able to restore cholesterol content in HCVcc almost to initial levels. When 4-cholestenone, cholesteryl acetate, 25-HC, DHC or 7-DHC was added to B-CD-treated HCVcc, virion-associated sterol levels were 146, 157, 68, 96 or 73 %, respectively, of that of the non-treated control. The proportion of cholesterol analogues to the total sterols incorporated was ⩾30 % when 4-cholestenone, cholesteryl acetate, DHC or 7-DHC was used; however, the proportion in the case of 25-HC was only 3 %. It may be that the hydrophilic modification of the aliphatic side chain leads to poor association with HCVcc.

Collectively, exogenous variants with the 3β-hydroxyl group, such as 4-cholestenone and cholesteryl acetate, can be incorporated into B-CD-treated HCVcc, but resulted in no recovery of virus infectivity, indicating the importance of the 3β-hydroxyl group of cholesterol associated with the virus envelope in HCV infectivity. In contrast, two variants with modification in their sterol ring structures, coprostanol and DHC, have the ability to substitute for cholesterol. However, 7-DHC, another variant within the sterol ring, is incorporated readily into the depleted virion and restores the virus density, HCV replenished with 7-DHC is not infectious. These facts suggest that reduced forms of the sterol ring (coprostanol and DHC) in virion-associated cholesterol can be permitted for maintaining virus infectivity. However, a molecule with an additional double bond in the ring structure (7-DHC) seems to fail to exhibit infectivity, presumably because the change reduces structural flexibility in the

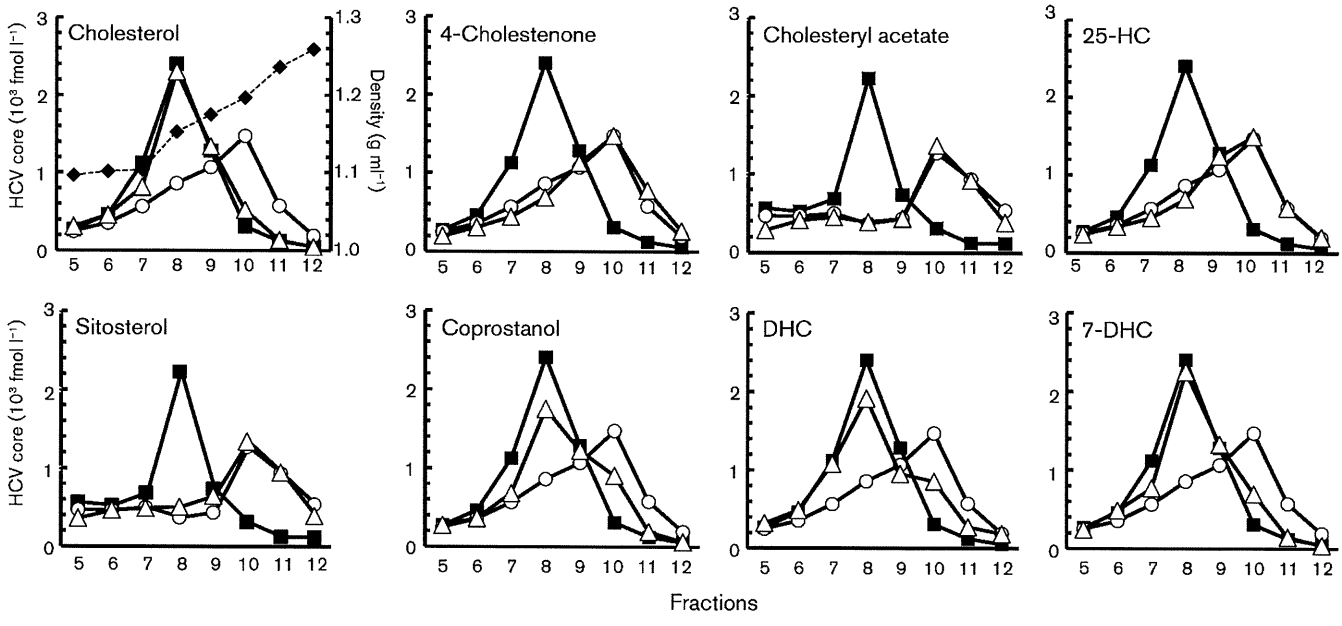

Fig. 2. Sucrose density-gradient profiles of lipid-modified HCV. Core protein concentration in each fraction of untreated HCVcc (■), B-CD-treated HCVcc (○) or HCVcc replenished with sterols (△) was determined. Corresponding densities of fractions are shown as a dashed line (◆).

sterol molecule and consequently in the virion structure. Coprostanol and DHC are *cis* and *trans* isomers, which are often known to have different physical properties. However, based on their molecular models, these two sterols, as well as cholesterol, possibly have similar spatial arrangements of the aliphatic side chain, the hydroxyl group and four-ring region because of their structural flexibility. In contrast, the spatial arrangement of 7-DHC does not seem comparable to that of cholesterol. Campbell *et al.* (2004) reported that replacement of HIV-1-associated cholesterol with raft-inhibiting sterols, including coprostanol, suppresses HIV-1 infectivity, whereas replacement with raft-promoting analogues such as DHC and 7-DHC (Megha *et al.*, 2006; Wang *et al.*, 2004; Xu & London, 2000; Xu *et al.*, 2001) maintains infectivity, demonstrating the importance of the raft-promoting properties of virion-associated cholesterol in HIV-1 infectivity (Campbell *et al.*, 2004). It is therefore likely that HCV-associated cholesterol is involved, at least in part, in virus infectivity via a molecular basis independent of lipid-raft formation.

The density of blood-circulating HCV is heterogeneous, ranging approximately from <1.06 to 1.25 g ml^{-1}, and it is proposed that low-density virus is associated with very-low-density lipoprotein (VLDL) and/or low-density lipoprotein (LDL) (André *et al.*, 2002; Thomssen *et al.*, 1993). It has recently been demonstrated that the pathway for VLDL assembly plays a role in assembly and maturation of infectious HCVcc (Icard *et al.*, 2009). HCVcc with low density, which is presumably associated with VLDL or VLDL-like lipoproteins, was found to possess higher infectivity than that with high density (Lindenbach *et al.*, 2006). This study, as well as our earlier work, indicated that removal of cholesterol from HCVcc by B-CD increased the buoyant density of the virus and reduced its infectivity. Thus, one may hypothesize that the virion-associated cholesterol plays a role in the formation of a complex with lipoproteins or apolipoproteins. To address this, the interaction between apolipoproteins and HCVcc with or without B-CD treatment was investigated by co-immunoprecipitation (Co-IP kit; Thermo Scientific). Virus samples were subjected separately to AminoLink Plus coupling resin, which was conjugated with a monoclonal antibody (mAb) against apolipoprotein E (ApoE) or apolipoprotein B (ApoB), and incubated at 4 °C for 4 h. After washing, total RNAs were extracted from the resulting resin beads by using TRIzol reagent (Invitrogen), followed by quantification of HCV RNA as described above (Takeuchi *et al.*, 1999). As indicated in Fig. 3(a), only a fraction of HCVcc was precipitated with an anti-ApoB mAb. In contrast, an anti-ApoE mAb was able to coprecipitate a considerable amount of the virus. It is of interest that B-CD-treated HCVcc hardly reacted with the mAb; however, the cholesterol-replenished virus was found to recover its reactivity, suggesting a role for virion-associated cholesterol in the formation of the HCV–lipoprotein/apolipoprotein complex. The results obtained are consistent with findings indicating that HCVcc can be captured with anti-ApoE antibodies, but capture with anti-ApoB antibodies is inefficient (Chang *et al.*, 2007; Hishiki *et al.*, 2010; Huang *et al.*, 2007; Jiang & Luo, 2009; Merz *et al.*, 2011; Nielsen *et al.*, 2006; Owen *et al.*, 2009), as well as with a recent model of structures of infectious HCV, in which HCVcc looks like ApoE-positive and primarily ApoB-negative lipoproteins (Bartenschlager *et al.*, 2011). We further tested the ApoE distribution in the density-gradient fractions of HCVcc samples (see Supplementary Fig. S1, available in JGV Online). With or without cholesterol depletion, ApoE was detected at a wide range of concentrations: 1.04 g ml^{-1} (fraction 1) to 1.17 g ml^{-1} (fraction 9). However, its level in the fractions at 1.10 g ml^{-1} (fraction 5) to approximately 1.17 g ml^{-1} was moderately decreased in the case of B-CD-treated virus.

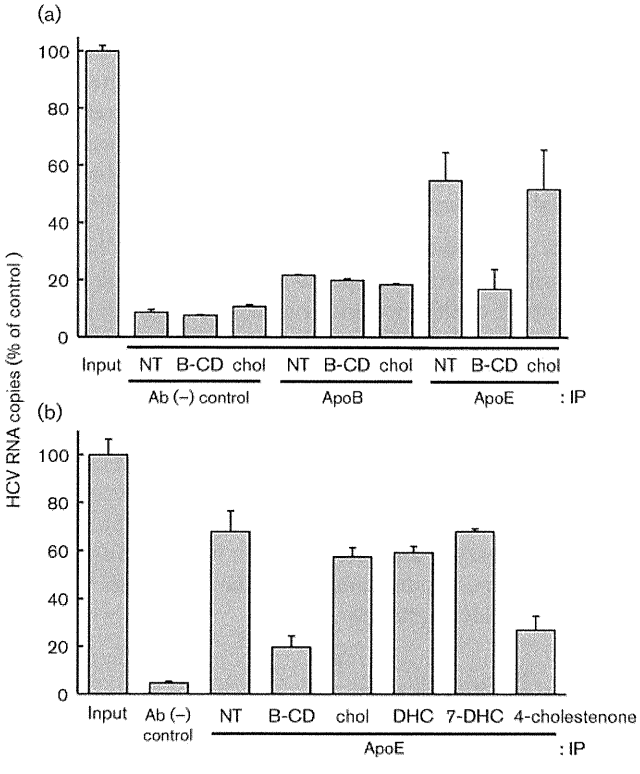

Fig. 3. Effect of virion-associated sterols on HCV–apolipoprotein interaction. (a) HCVcc samples with no treatment (NT), B-CD-treated (B-CD) or replenished with cholesterol (chol) were incubated with an amine-reactive resin coupling either an anti-ApoB mAb (ApoB) or an anti-ApoE mAb (ApoE). Control resin that is composed of the same material as above, but is not activated, was used as a negative control [Ab (–) control]. (b) B-CD-treated HCVcc was incubated with cholesterol (chol), DHC, 7-DHC or 4-cholestenone, followed by immunoprecipitation with the resin coupling with anti-ApoE mAb. (a, b) HCV RNAs in the immunoprecipitates were quantified and are indicated as percentages of the amount of input HCVcc RNA. Means+SD of three samples are shown. Data are representative of three experiments.

Whether cholesterol analogues could have a comparable role in HCV association with lipoprotein was examined further (Fig. 3b). Addition of DHC or 7-DHC, but not 4-cholestenone, to B-CD-treated HCVcc resulted in the recovery of coprecipitation of the virus with anti-ApoE. The results are correlated with the effect of sterols on the restoration of the buoyant densities of lipid-modified HCVcc (Fig. 2), suggesting that virion-associated cholesterol variants with modification in the sterol rings, but not in either the 3β-hydroxyl group or the aliphatic side chain, may tolerate the interaction between HCV and ApoE-positive lipoprotein.

Given that 7-DHC restored the association of HCV with ApoE and virion buoyant density, but did not restore infectivity, cholesterol and/or its analogues might affect the ability of virion membranes to fuse with the cell, independent of ApoE association. As cholesterol is an important mediator of membrane fluidity, one may hypothesize that HCV-associated cholesterol is involved in infectivity through modulation of the membrane fluidity. It has been reported that, in patients with Smith–Lemli–Opitz syndrome, a disorder of the cholesterol-synthesis pathway, cholesterol content decreases and 7-DHC increases in the cell membranes, leading to alteration of phospholipid packing in the membrane and abnormal membrane fluidity (Tulenko *et al.*, 2006).

It is now accepted that maturation and release of infectious HCV coincide with the pathway for producing VLDLs, which export cholesterol and triglyceride from hepatocytes. This study revealed roles for the structural basis of virion-associated cholesterol in the infectivity, buoyant density and apolipoprotein association of HCV. Although it was shown that HCV virions in infected patients, so-called lipo–viro particles, exhibited certain biochemical properties such as containing ApoB, ApoC and ApoE (Diaz *et al.*, 2006; Bartenschlager *et al.*, 2011), our studies provide useful information and the basis for future investigations toward a deeper understanding of the biogenesis pathway of infectious HCV particles.

Acknowledgements

We thank M. Matsuda, M. Sasaki and T. Date for technical assistance and T. Mizoguchi for secretarial work. This work was partially supported by a grant-in-aid for Scientific Research from the Japan Society for the Promotion of Science, from the Ministry of Health, Labor, and Welfare of Japan, and from the Ministry of Education, Culture, Sports, Science, and Technology.

References

Aizaki, H., Morikawa, K., Fukasawa, M., Hara, H., Inoue, Y., Tani, H., Saito, K., Nishijima, M., Hanada, K. & other authors (2008). Critical role of virion-associated cholesterol and sphingolipid in hepatitis C virus infection. *J Virol* **82**, 5715–5724.

Akazawa, D., Date, T., Morikawa, K., Murayama, A., Miyamoto, M., Kaga, M., Barth, H., Baumert, T. F., Dubuisson, J. & Wakita, T. (2007). CD81 expression is important for the permissiveness of Huh7 cell clones for heterogeneous hepatitis C virus infection. *J Virol* **81**, 5036–5045.

André, P., Komurian-Pradel, F., Deforges, S., Perret, M., Berland, J. L., Sodoyer, M., Pol, S., Bréchot, C., Paranhos-Baccalà, G. & Lotteau, V. (2002). Characterization of low- and very-low-density hepatitis C virus RNA-containing particles. *J Virol* **76**, 6919–6928.

Bartenschlager, R., Penin, F., Lohmann, V. & André, P. (2011). Assembly of infectious hepatitis C virus particles. *Trends Microbiol* **19**, 95–103.

Bremer, C. M., Bung, C., Kott, N., Hardt, M. & Glebe, D. (2009). Hepatitis B virus infection is dependent on cholesterol in the viral envelope. *Cell Microbiol* **11**, 249–260.

Campbell, S. M., Crowe, S. M. & Mak, J. (2001). Lipid rafts and HIV-1: from viral entry to assembly of progeny virions. *J Clin Virol* **22**, 217–227.

Campbell, S. M., Crowe, S. M. & Mak, J. (2002). Virion-associated cholesterol is critical for the maintenance of HIV-1 structure and infectivity. *AIDS* **16**, 2253–2261.

Campbell, S., Gaus, K., Bittman, R., Jessup, W., Crowe, S. & Mak, J. (2004). The raft-promoting property of virion-associated cholesterol, but not the presence of virion-associated Brij 98 rafts, is a determinant of human immunodeficiency virus type 1 infectivity. *J Virol* **78**, 10556–10565.

Chang, K. S., Jiang, J., Cai, Z. & Luo, G. (2007). Human apolipoprotein E is required for infectivity and production of hepatitis C virus in cell culture. *J Virol* **81**, 13783–13793.

Diaz, O., Delers, F., Maynard, M., Demignot, S., Zoulim, F., Chambaz, J., Trépo, C., Lotteau, V. & André, P. (2006). Preferential association of hepatitis C virus with apolipoprotein B48-containing lipoproteins. *J Gen Virol* **87**, 2983–2991.

Graham, D. R., Chertova, E., Hilburn, J. M., Arthur, L. O. & Hildreth, J. E. (2003). Cholesterol depletion of human immunodeficiency virus type 1 and simian immunodeficiency virus with β-cyclodextrin inactivates and permeabilizes the virions: evidence for virion-associated lipid rafts. *J Virol* **77**, 8237–8248.

Hambleton, S., Steinberg, S. P., Gershon, M. D. & Gershon, A. A. (2007). Cholesterol dependence of varicella-zoster virion entry into target cells. *J Virol* **81**, 7548–7558.

Hishiki, T., Shimizu, Y., Tobita, R., Sugiyama, K., Ogawa, K., Funami, K., Ohsaki, Y., Fujimoto, T., Takaku, H. & other authors (2010). Infectivity of hepatitis C virus is influenced by association with apolipoprotein E isoforms. *J Virol* **84**, 12048–12057.

Huang, H., Sun, F., Owen, D. M., Li, W., Chen, Y., Gale, M., Jr & Ye, J. (2007). Hepatitis C virus production by human hepatocytes dependent on assembly and secretion of very low-density lipoproteins. *Proc Natl Acad Sci U S A* **104**, 5848–5853.

Icard, V., Diaz, O., Scholtes, C., Perrin-Cocon, L., Ramière, C., Bartenschlager, R., Penin, F., Lotteau, V. & André, P. (2009). Secretion of hepatitis C virus envelope glycoproteins depends on assembly of apolipoprotein B positive lipoproteins. *PLoS One* **4**, e4233.

Jiang, J. & Luo, G. (2009). Apolipoprotein E but not B is required for the formation of infectious hepatitis C virus particles. *J Virol* **83**, 12680–12691.

Lindenbach, B. D., Meuleman, P., Ploss, A., Vanwolleghem, T., Syder, A. J., McKeating, J. A., Lanford, R. E., Feinstone, S. M., Major, M. E. & other authors (2006). Cell culture-grown hepatitis C virus is infectious *in vivo* and can be recultured *in vitro*. *Proc Natl Acad Sci U S A* **103**, 3805–3809.

Megha, Bakht, O. & London, E. (2006). Cholesterol precursors stabilize ordinary and ceramide-rich ordered lipid domains (lipid

rafts) to different degrees. Implications for the Bloch hypothesis and sterol biosynthesis disorders. *J Biol Chem* **281**, 21903–21913.

Merz, A., Long, G., Hiet, M. S., Brügger, B., Chlanda, P., Andre, P., Wieland, F., Krijnse-Locker, J. & Bartenschlager, R. (2011). Biochemical and morphological properties of hepatitis C virus particles and determination of their lipidome. *J Biol Chem* **286**, 3018–3032.

Nielsen, S. U., Bassendine, M. F., Burt, A. D., Martin, C., Pumeechockchai, W. & Toms, G. L. (2006). Association between hepatitis C virus and very-low-density lipoprotein (VLDL)/LDL analyzed in iodixanol density gradients. *J Virol* **80**, 2418–2428.

Owen, D. M., Huang, H., Ye, J. & Gale, M., Jr (2009). Apolipoprotein E on hepatitis C virion facilitates infection through interaction with low-density lipoprotein receptor. *Virology* **394**, 99–108.

Takeuchi, T., Katsume, A., Tanaka, T., Abe, A., Inoue, K., Tsukiyama-Kohara, K., Kawaguchi, R., Tanaka, S. & Kohara, M. (1999). Real-time detection system for quantification of hepatitis C virus genome. *Gastroenterology* **116**, 636–642.

Thomssen, R., Bonk, S. & Thiele, A. (1993). Density heterogeneities of hepatitis C virus in human sera due to the binding of beta-lipoproteins and immunoglobulins. *Med Microbiol Immunol (Berl)* **182**, 329–334.

Tulenko, T. N., Boeze-Battaglia, K., Mason, R. P., Tint, G. S., Steiner, R. D., Connor, W. E. & Labelle, E. F. (2006). A membrane defect in the pathogenesis of the Smith–Lemli–Opitz syndrome. *J Lipid Res* **47**, 134–143.

Wakita, T., Pietschmann, T., Kato, T., Date, T., Miyamoto, M., Zhao, Z., Murthy, K., Habermann, A., Kräusslich, H. G. & other authors (2005). Production of infectious hepatitis C virus in tissue culture from a cloned viral genome. *Nat Med* **11**, 791–796.

Wang, J., Megha & London, E. (2004). Relationship between sterol/steroid structure and participation in ordered lipid domains (lipid rafts): implications for lipid raft structure and function. *Biochemistry* **43**, 1010–1018.

Xu, X. & London, E. (2000). The effect of sterol structure on membrane lipid domains reveals how cholesterol can induce lipid domain formation. *Biochemistry* **39**, 843–849.

Xu, X., Bittman, R., Duportail, G., Heissler, D., Vilcheze, C. & London, E. (2001). Effect of the structure of natural sterols and sphingolipids on the formation of ordered sphingolipid/sterol domains (rafts). Comparison of cholesterol to plant, fungal, and disease-associated sterols and comparison of sphingomyelin, cerebrosides, and ceramide. *J Biol Chem* **276**, 33540–33546.

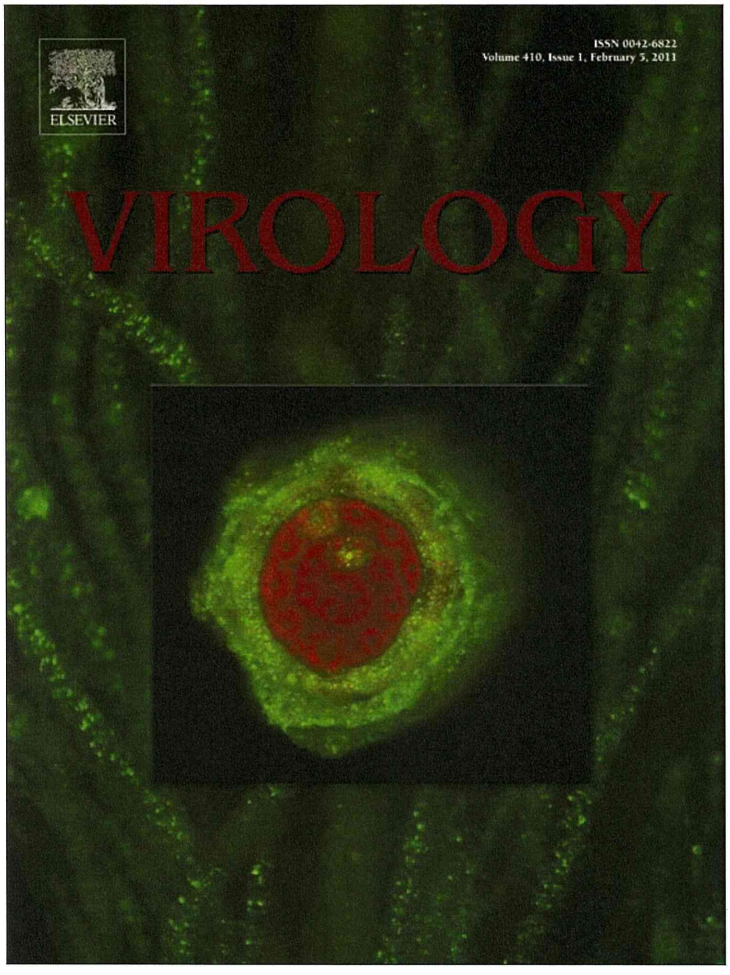

Virology 410 (2011) 38–47

Contents lists available at ScienceDirect

Virology

journal homepage: www.elsevier.com/locate/yviro

Chaperonin TRiC/CCT participates in replication of hepatitis C virus genome via interaction with the viral NS5B protein

Yasushi Inoue [a,b,c], Hideki Aizaki [a], Hiromichi Hara [a], Mami Matsuda [a], Tomomi Ando [a], Tetsu Shimoji [a], Kyoko Murakami [a], Takahiro Masaki [a], Ikuo Shoji [d], Sakae Homma [b], Yoshiharu Matsuura [e], Tatsuo Miyamura [a], Takaji Wakita [a], Tetsuro Suzuki [a,f,*]

[a] Department of Virology II, National Institute of Infectious Diseases, Tokyo 162-8640, Japan
[b] Department of Respiratory Medicine, Toho University School of Medicine, Tokyo 143-8541, Japan
[c] International University of Health and Welfare, Mita Hospital, Tokyo 108-8329, Japan
[d] Division of Microbiology, Kobe University Graduate School of Medicine, Hyogo 650-0017, Japan
[e] Research Institute for Microbial Diseases, Osaka University, Osaka 565-0871, Japan
[f] Department of Infectious Diseases, Hamamatsu University School of Medicine, Hamamatsu 431-3192, Japan

ARTICLE INFO

Article history:
Received 12 June 2010
Returned to author for revision 18 July 2010
Accepted 15 October 2010
Available online 18 November 2010

Keywords:
Hepatitis C virus
Replication
Non-structural protein
Chaperonin

ABSTRACT

To identify the host factors implicated in the regulation of hepatitis C virus (HCV) genome replication, we performed comparative proteome analyses of HCV replication complex (RC)-rich membrane fractions prepared from cells harboring genome-length bicistronic HCV RNA at the exponential and stationary growth phases. We found that the eukaryotic chaperonin T-complex polypeptide 1 (TCP1)-ring complex/chaperonin-containing TCP1 (TRiC/CCT) plays a role in the replication possibly through an interaction between subunit CCT5 and the viral RNA polymerase NS5B. siRNA-mediated knockdown of CCT5 suppressed RNA replication and production of the infectious virus. Gain-of-function activity was shown following co-transfection with whole eight TRiC/CCT subunits. HCV RNA synthesis was inhibited by an anti-CCT5 antibody in a cell-free assay. These suggest that recruitment of the chaperonin by the viral nonstructural proteins to the RC, which potentially facilitate folding of the RC component(s) into the mature active form, may be important for efficient replication of the HCV genome.

Introduction

Hepatitis C virus (HCV) is a major cause of chronic liver diseases, such as chronic hepatitis, hepatic steatosis, cirrhosis, and hepatocellular carcinoma (Hoofnagle, 2002; Manns et al., 2006; Saito et al., 1990; Seeff and Hoofnagle, 2003). HCV is an enveloped positive-strand RNA virus belonging to the *Hepacivirus* genus of the Flaviviridae family. Its genome of ~9.6 kb encodes a polyprotein precursor of ~3000 amino acids (aa) (Suzuki et al., 2007; Taguwa et al., 2008). The precursor polyprotein is post- or cotranslationally processed by both viral and host proteases into at least ten viral products. The nonstructural (NS) proteins NS3–NS5B are necessary and sufficient for autonomous HCV RNA replication. They form a membrane-associated replication complex (RC), in which NS5B is the RNA-dependent RNA polymerase (RdRp) that is responsible for copying the RNA genome of the virus during replication. The HCV RC has been detected in detergent-resistant membrane (DRM) structures, possibly in a lipid-raft structure (Aizaki et al., 2004; Shi et al., 2003). Cell-free RC replication activity has also been demonstrated in crude membrane fractions of HCV subgenomic replicon cells (Aizaki et al., 2004; Ali et al., 2002; Hara et al., 2009; Hardy et al., 2003; Yang et al., 2004); these cell-free systems provide semi-intact RdRp assays for biochemical dissection of viral replication.

In general, any process that occurs during viral replication is dependent on the host cell machinery and requires close interaction between viral and cellular proteins. Although evidence that host cell factors interact with HCV NS proteins and are involved in viral replication is accumulating (Moriishi and Matsuura, 2007), the cellular components of HCV RC and their functional roles in viral replication are not fully understood.

Recently, using comparative proteome analysis, we identified 27 cellular proteins that were highly enriched in the DRM fraction of HCV replicon cells relative to parental cells. Subsequent analyses demonstrated that one of the identified proteins, creatine kinase B, a key ATP-generating enzyme, is important for efficient replication of the HCV genome and for production of the infectious virus (Hara et al., 2009).

In this study, to extend our investigation and to increase our understanding of the precise components of HCV RC and the

* Corresponding author. Department of Infectious Diseases, Hamamatsu University School of Medicine, Hamamatsu 431-3192, Japan. Fax: +81 53 435 2337.
E-mail address: tesuzuki@hama-med.ac.jp (T. Suzuki).

0042-6822/$ – see front matter © 2010 Elsevier Inc. All rights reserved.
doi:10.1016/j.virol.2010.10.026

mechanisms of viral genome replication, we designed another comparative proteomic approach in which cells harboring genome-length bicistronic HCV RNA at the exponential growth phase (showing rapid replication of viral RNA) were compared with cells at the confluent-growth phase (showing poor replication of viral RNA). This strategy revealed that the chaperonin T-complex polypeptide (TCP1)-ring complex/chaperonin-containing TCP1 (TRiC/CCT) participates in HCV RNA replication and virion production possibly through an interaction between CCT5 (chaperonin-containing TCP1, subunit 5) and NS5B.

Results

CCT5 and Hsc70 are enriched in the DRM fraction containing the HCV RC

Recently, we analyzed the protein content of DRM fractions prepared from HCV subgenomic replicons and parental Huh-7 cells and identified 27 cellular proteins that were enriched in the DRM fraction prepared from the replicon cells (Hara et al., 2009). These were identified as factors that may be involved in the HCV RC and in viral replication. In fact, subsequent silencing of several genes coding for these proteins resulted in the inhibition of HCV RNA replication (Hara et al., 2009). However, it is likely that proteins unrelated to HCV replication are also included in the identified groups because long-term culture of the replicon cells under the selective pressure of G418 selects for a subpopulation of the parental cells and may induce changes in their protein expression profiles. Thus, to minimize interline differences in culture background, we further designed a comparative proteome analysis using a single cell line as follows.

HCV replication efficiency is dependent on the conditions of host cell growth. High cell density of the replicon culture has a reversible inhibitory effect on viral replication (Nelson and Tang, 2006; Pietschmann et al., 2001). Fig. 1A demonstrates that a high level of HCV RNA was detected in cells harboring the genome-length bicistronic HCV RNA, Con1 strain of genotype 1b (RCYM1) in the growth phase, whereas the RNA level declined sharply when the cells reached the stationary phase. We further compared the synthesis of HCV RNA in cell-free reaction mixtures containing the viral RC isolated from the RCYM1 cells at various cell densities (Fig. 1B). Replication activity was highest at the mid-log phase of cell growth (day 4 after seeding). By contrast, little or no RNA synthesis was observed under the confluent-growth cell culture (day 8), confirming the critical role of host cell growth conditions in the replication of the HCV genome.

Thus, to identify the host cell proteins required for HCV replication, we designed a two-dimensional fluorescence difference gel electrophoresis (2D-DIGE)-based comparative proteomics analysis of RC-rich DRM fractions prepared from RCYM1 cells at the mid-log and confluent-growth phases. Protein spots that reproducibly showed a greater than 1.5-fold difference in the mid-log growth- and the confluent phases were excised and digested by trypsin or lysylendopeptidase. Matrix-assisted laser desorption ionization–time-of-flight (MALDI-TOF) mass spectrometry (MS), which allows identification of the corresponding proteins in 9 cases (Table 1). Two increased spots that showed an increase in levels (their stereoscopic images are shown in Fig. 2A) were identified as CCT5 and Hsc70. CCT5, an epsilon subunit of chaperonin TRiC/CCT, is a 900-kDa toroid-shaped complex consisting of eight different subunits (Valpuesta et al., 2002; Yaffe et al., 1992). Hsc70, a member of the HSP70 family, is a 71-kDa heat shock cognate protein (Dworniczak and Mirault, 1987). Independent of the proteome analyses, DRM fractions and whole cell lysates were prepared from RCYM1 cells at two different growth phases (as above) and were analyzed by immunoblotting (Fig. 2B). Steady-state levels of CCT5 and Hsc70 were obviously higher in the DRM fraction prepared from the cells that were at the mid-log growth phase compared with those at the confluent phase. However, in the whole cell analyses, they were shown to be present at comparable levels during the two different growth phases. These results suggest that expression of CCT5 and Hsc70 is not enhanced in proliferating cells and that the enrichment of these proteins in the DRM fraction is possibly due to their post-translational modification. It should be noted that in the previous proteome analysis, CCT5 and other TRiC/CCT subunits, such as CCT1 and CCT2, were identified as proteins that were enriched in the DRM fraction prepared from subgenomic replicon-containing cells compared with that prepared from parental cells (Hara et al., 2009). We showed that CCT5 and CCT1 were enriched in the DRM fractions of cells transfected with the HCV genomic RNA derived from JFH-1 isolate as well as of subgenomic replicon cells (Fig. 2C).

TRiC/CCT participates in replication of the HCV genome

We investigated gain- and loss-of-functions of TRiC/CCT and Hsc70 with respect to the replication of HCV RNA. Seventy-two hours after RCYM1 cells were transfected with eight plasmids corresponding to each of the TRiC/CCT subunits, the level of HCV RNA in the cells (determined by quantitative RT-PCR) significantly increased to 2-fold that observed in the control cells. However, exogenous expression of Hsc70 in the RCYM1 cells showed no effect on the viral RNA (Fig. 3A). siRNAs targeted to CCT5 or Hsc70 and consisting of pools of three target-specific siRNAs or control nonspecific siRNAs were transfected

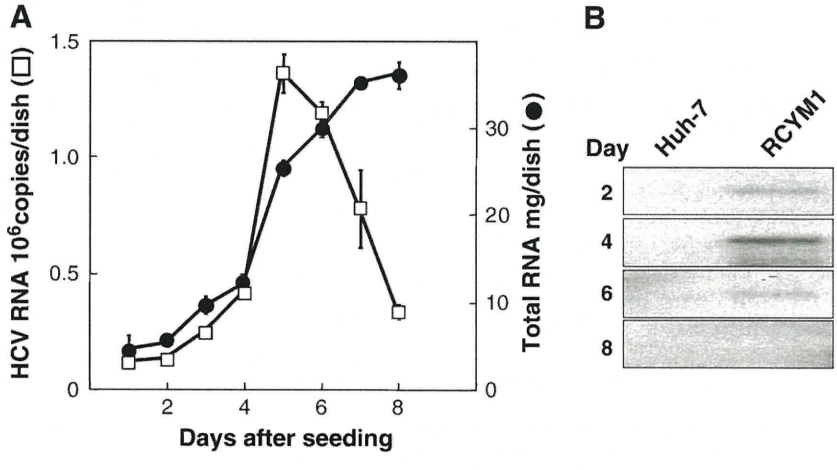

Fig. 1. Effect of cell growth on HCV RNA replication. (A) Measurement of HCV RNA (open squares) and total cellular RNA (closed circles) in RCYM1 cells at the time of harvest (days after seeding). (B) DRM fractions obtained from RCYM1 and parental Huh-7 cells harvested as indicated (day) were analyzed by cell-free RNA replication assay. RNA extracted from each sample was analyzed by agarose gel electrophoresis and autoradiograph.

Table 1
Selected cellular proteins that reproducibly increased and decreased in membrane fraction of RCYM1 cells at exponential growth phase.

Av. ratio	T-test	Coverage (%)	Protein name	Molecular function	GI
Increased proteins					
1.58	0.017	31	CCT5	Protein folding	33879913
1.54	0.005	35	HSPA8 (Hsc70)	Protein folding	24657660
Decreased proteins					
−1.95	0.028	44	Creatine kinase isozyme CK-B gene, exon 8	Energy pathway/metabolism	180568
−1.53	0.011	16	Chain C, Human Sirt2 Histone deacetylase	Cell cycle control	15826438
−2.14	0.001	33	Proteasome regulatory particle subunit p44S10	Metabolism	15341748
−1.71	0.004	21	Aldehyde dehydrogenase	Metabolism	178388
−1.85	0.004	40	Aminoacylase 1	Metabolism	12804328
−2.77	0.003	15	Eukaryotic translation initiation factor 3, subunit 3 gamma	Metabolism (translation regulator activity)	6685512
−2.43	0.014	20	Intraflagellar transport protein 74 homolog (Coiled-coil domain-containing protein 2)	Cell growth and/or maintenance	10439078

Three paired samples of RC-rich membrane fractions at the exponential- and confluent-growth phases of RCYM1 cultures were analyzed. The proteins representing a more than 1.5-fold increase or decrease (−) reproducibly and significantly are indicated.
Coverage (%): the ratio of the portion of protein sequence covered by matched peptides to the whole sequence.
GI: GenInfo Identifier number.

into RCYM1 cells. After 72 h, the HCV RNA level was reduced by 42% and 27% in the cells transfected with siRNAs against CCT5 and Hsc70, respectively, compared with controls (Fig. 3B). TRiC/CCT possibly interacts with Hsc70, and its complex formation contributes to increasing the efficiency of protein folding (Cuéllar et al., 2008). Our results suggest the involvement of TRiC/CCT and Hsc70 in the HCV life cycle. In particular, TRiC/CCT may play an important role in the replication of the viral genome.

To verify the specificity of the knockdown of CCT5 siRNA, we further synthesized two siRNAs targeted to different regions used in the above CCT5 siRNA and assessed their knockdown effect on HCV genome replication (Fig. 3C, upper panel). As expected, transfection of

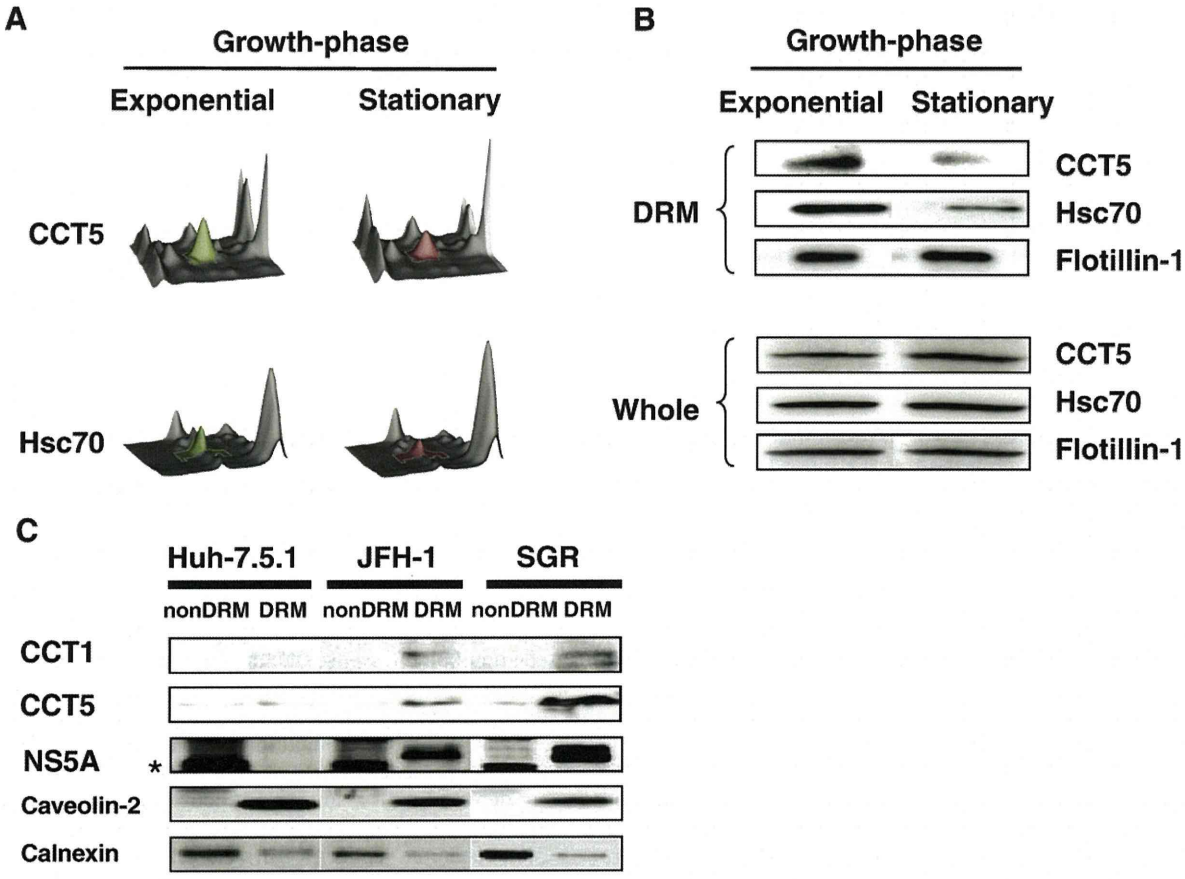

Fig. 2. Comparison of protein levels in DRM fractions prepared from RCYM1 cells at the exponential and stationary growth phases. (A) Three-dimensional images of CCT5 and Hsc70 analyzed by Ettan DIGE (GE Healthcare). Spots corresponding to CCT5/Hsc70 at exponential and stationary growth phases of the cells, respectively, are shown in green and red. (B) Equal amounts of protein in the DRM fractions prepared from RCYM1 cells at the exponential and stationary growth phases or corresponding whole cell lysates were analyzed by immunoblotting with Abs against CCT5, Hsc70 or flotillin-1. (C) Enrichment of CCT1 and CCT5 in the DRM fractions of HCV RNA replicating cells. Equal amounts of DRM or non-DRM fractions from full-length JFH-1 RNA transfected cells (JFH-1), subgenomic replicon cells (SGR) and parental Huh-7.5.1 cells were analyzed by immunoblotting with antibodies against CCT1, CCT5, NS5A, caveolin-2 or calnexin. *Non-specific bands.

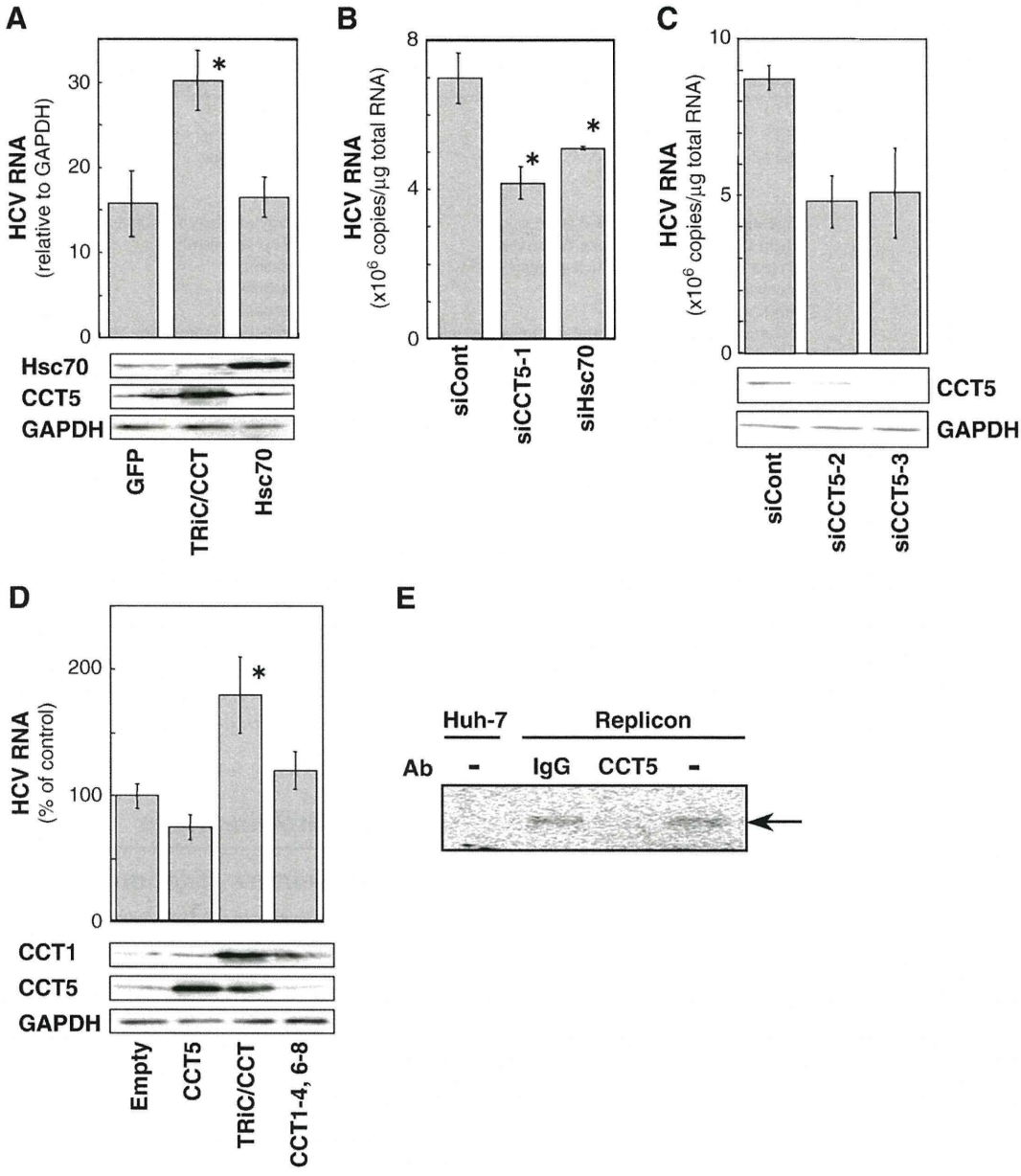

Fig. 3. Involvement of TRiC/CCT in HCV replication (A and D). Overexpression of all eight subunits of TRiC/CCT (TRiC/CCT); seven subunits, CCT1, 2, 3, 4, 6, 7, and 8 (CCT1–4, 6–8); subunit CCT5 only (CCT5); Hsc70; or control GFP in RCYM1 cells. HCV RNA levels were determined 48 h post-transfection (B and C). Knockdown of endogenous CCT5 or Hsc70 in RCYM1 cells, which were transfected with three types of siRNAs against CCT5 (siCCT5-1, -2, and -3), siRNA against Hsc70 (siHsc70), or control siRNA (siCont), and were harvested at 72 h post-transfection. siCCT5-1 and siHsc70 consisted of pools of three target-specific siRNAs. Immunoblotting for CCT1, CCT5, Hsc70 and GAPDH was performed (A, C and D; lower). (E) Cell-free de novo viral RNA synthesis assays were performed in the presence of anti-CCT5 Ab or control mouse IgG. Cytoplasmic fractions from SGR-N (replicon) and parental Huh-7 cells were used. An arrow indicates the synthesized HCV RNA. Error bars denote standard deviations with asterisks indicating statistical significance (*$P<0.01$).

RCYM1 cells with each CCT5 siRNA resulted in a reduction in viral RNA to a level of about 50% of that observed in cells treated with control siRNAs. Immunoblotting confirmed the efficient reduction in expression of endogenous CCT5 and the lack of cytotoxic effect exerted by the CCT5 siRNAs (Fig. 3C, middle and lower panels).

Having confirmed the upregulation of HCV RNA by ectopic expression of all the TRiC/CCT subunits, we further addressed the possibility that CCT5, independent of the complete TRiC/CCT complex, might have a role in promoting replication of HCV RNA. Transfection with either a CCT5 expression plasmid alone or with seven plasmids expressing all the TRiC/CCT subunits except CCT5 resulted in no or only a slight increase in the level of HCV RNA, indicating that all CCT subunits are required for HCV replication (Fig. 3D).

TRiC/CCT is generally known as a cytosolic chaperone (Valpuesta et al., 2002). However, it is enriched in the DRM fraction of HCV-replicating cells during the exponential growth phase (Fig. 2B). We used immunofluorescence staining to investigate whether TRiC/CCT is localized in the intracellular membrane compartments where replication of the viral genome occurs (Fig. 4). The de novo-synthesized RdRp was labeled by bromouridine triphosphate (BrUTP) incorporation in the presence of actinomycin D, and brominated nucleotides were detected with a specific antibody (Ab). Fluorescence staining in distinct speckles of various sizes was found in the cytoplasm of the HCV subgenomic replicon cells, whereas no signal was detected in the control cells, indicating that the observed BrUTP-incorporating RNA is mostly viral, newly synthesized viral RNA (Fig. 4A). Double immunofluorescence staining showed that a certain section of CCT5 co-distributed with the BrUTP-labeled RNA (Fig. 4A), which is known to co-exist with HCV NS proteins in viral replicating cells (Shi et al., 2003). We further observed that CCT5 was at least partially colocalized

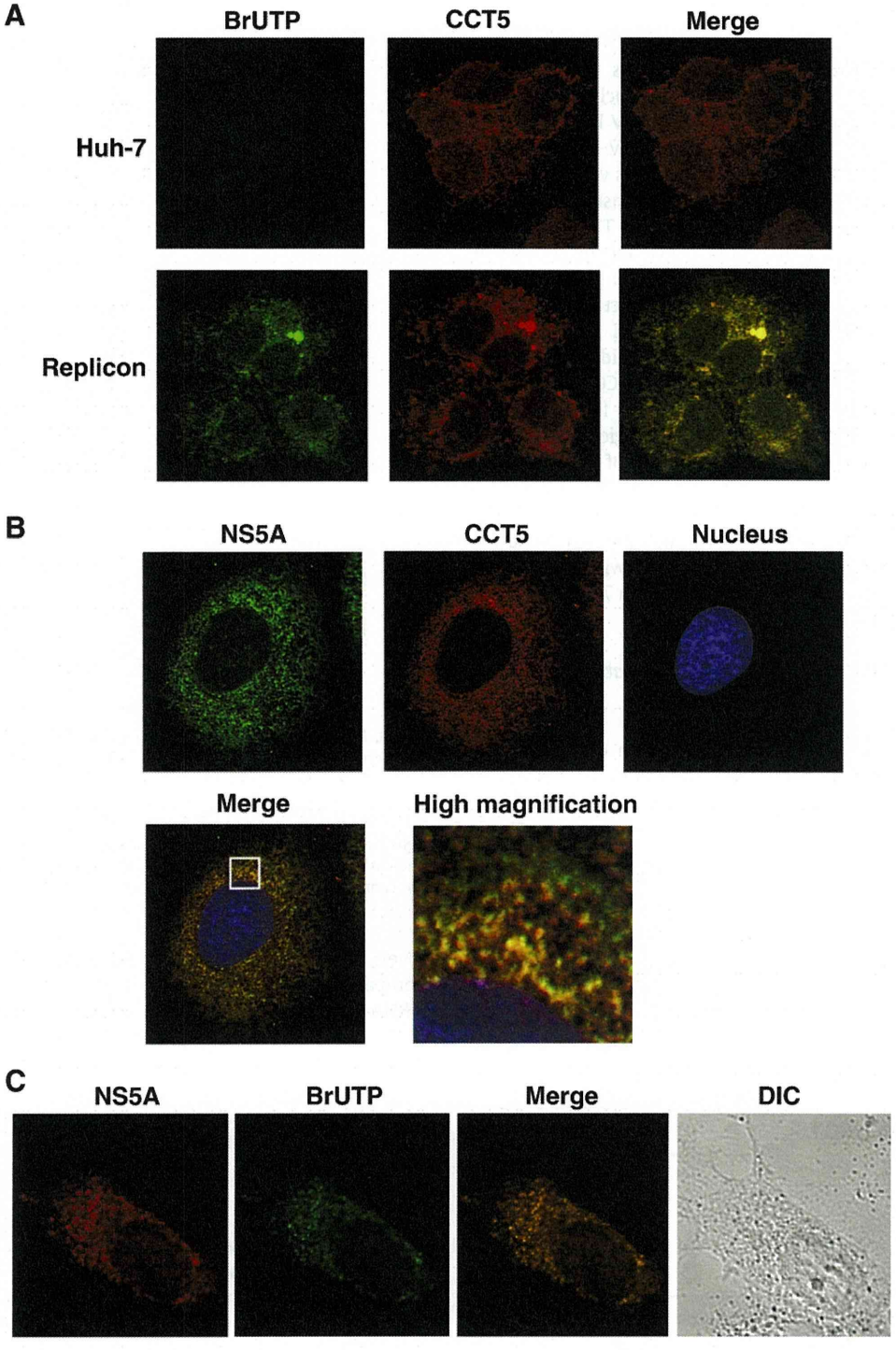

Fig. 4. Immunofluorescence analysis of CCT5 in SGR-N and Huh-7 cells (A) and HCVcc-infected cells (B). The primary Abs used were anti-CCT5 goat polyclonal Ab (red), anti-BrUTP monoclonal Ab (green), and anti-NS5A monoclonal Ab (green). Merged images of red and green signals (A) or of red, green and blue (nucleus) signals (B) are shown. The high magnification panel is an enlarged image of a white square of the merge panel. (C) Colocalization of NS5A protein with the viral RNA. The replicon cells were permeabilized with lysolecithin and labeled with BrUTP, followed by staining with anti-NS5A rabbit polyclonal Ab (red) and the anti-BrUTP monoclonal Ab (green). DIC, differential interference contrast.

with the viral NS protein in certain compartments sharing a dot-like structure in Huh-7 cells infected with HCV JFH-1 infectious HCV (HCVcc) derived from HCV genotype 2a (Fig. 4B) as well as in the replicon cells (data not shown). Fig. 4C indicated co-localization of BrUTP-labeled RNA with NS5A.

To further address the role of TRiC/CCT in HCV genome replication, we performed immunodepletion and in vitro replication analyses, which have been used for studying the genome replication of several viruses (Daikoku et al., 2006; Garcin et al., 1993; Liu et al., 2009). Cell extracts prepared from the HCV-replicating cells were reacted with either a mouse monoclonal Ab against CCT5 or mouse IgG derived from preimmune serum, followed by cell-free synthesis of HCV RNA. Fig. 3E shows that treatment with anti-CCT5 Ab inhibited viral RNA synthesis, whereas the control IgG did not affect the process, suggesting that TRiC/CCT participates directly in HCV RNA replication.

CCT5 interacts with HCV NS5B

The genome replication machinery of HCV is a membrane-associated complex composed of multiple factors including viral NS proteins. Given the involvement of TRiC/CCT in HCV RNA synthesis, we next examined its possible interaction with HCV NS proteins. A first attempt to immunoprecipitate the viral proteins with antibodies against TRiC/CCT subunits in the replicon cells was unsuccessful (data not shown), suggesting that endogenous levels of TRiC/CCT is not sufficient to pull out NS5B. Next, dual (myc/FLAG)-tagged NS3, NS5A, or NS5B proteins derived from the genotype 1b NIHJ1 strain were co-expressed with CCT5 in Huh-7 cells and then subjected to two-step immunoprecipitation with anti-myc and anti-FLAG Abs (Ichimura et al., 2005; Shirakura et al., 2007). An empty plasmid was used as a negative control in the analyses. As shown in Fig. 5A, CCT5 specifically interacted with NS5B. Little or no interaction was found between CCT5 and NS3 or NS5A. To determine the NS5B region required for the interaction with CCT5, various deletion mutants of HA-NS5B were constructed and their interactions with CCT5 were analyzed as described above. CCT5 was shown to be coimmunoprecipitated with either a full-length NS5B (aa 1–591), an N-terminal deletion (aa 71–591) or a C-terminal deletion (aa 1–570), but not with deletions aa 215–591 or aa 320–591 (Fig. 5B), suggesting that aa 71–214 of NS5B are important for its interaction with CCT5.

Knockdown of CCT5 results in the reduction of propagation of infectious HCV

We further examined whether the knockdown of CCT5 would abrogate the production of infectious HCV (HCVcc), derived from JFH-1 (Fig. 6). At 72 h post-transfection with each CCT5 siRNA, HCV RNA

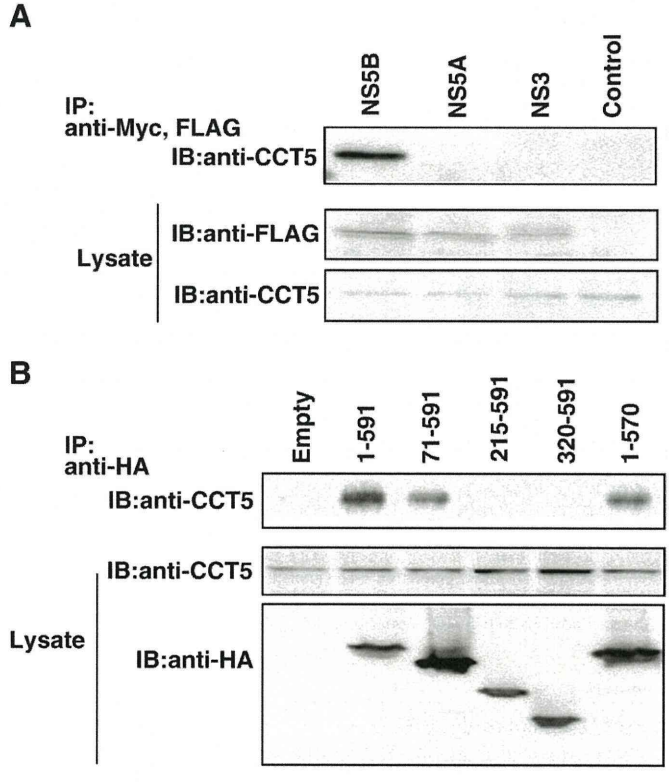

Fig. 5. CCT5 interacts with HCV NS5B. (A) CCT5 was co-expressed with MEF-tagged-NS5B, -NS5A, or -NS3 protein of strain NIHJ1 in cells, followed by two-step immunoprecipitation (IP) with anti-FLAG and anti-myc Abs. Immunoprecipitates were subjected to immunoblotting with anti-CCT5 Ab (IB). (B) Full-length NS5B (1–591) or its deletions (71–591, 215–591, 320–591, 1–570) along with a HA tag were co-expressed with CCT5. IP and IB were performed as described above.

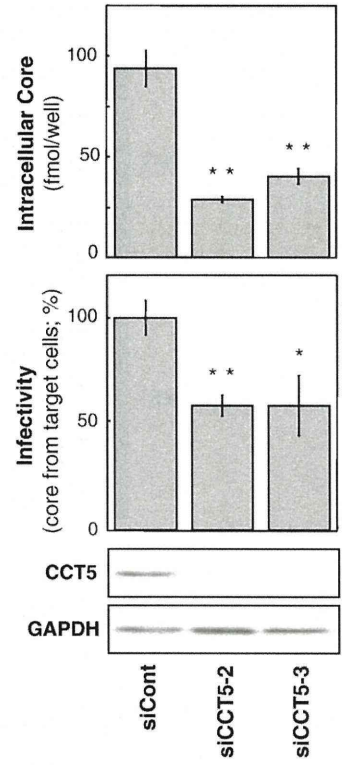

Fig. 6. Knockdown of endogenous CCT5 in HCVcc-infected cells. The cells were transfected with siRNAs against CCT5 (siCCT5-2, -3) or with control siRNAs (siCont). At 72 h post-transfection, the viral core protein levels in cells were determined (upper panel). Collected culture supernatants were inoculated into naïve Huh7.5.1 cells and intracellular core proteins were determined at 72 h post-infection (middle panel). Cells transfected with siRNAs were analyzed by immunoblotting with anti-CCT5 or anti-GAPDH Ab (lower panel). Error bars denote standard deviations with asterisks indicating statistical significance (*$P<0.05$; **$P<0.01$).

levels in Huh-7 cells infected with HCVcc were reduced by 25–35% compared with controls. Accordingly, virion production from CCT5 siRNA-transfected cultures was significantly decreased, as determined by intracellular HCV core protein levels at 72 h after the infection of naïve cells with culture supernatants taken from transfected cells. These results demonstrate that reduction of the HCV RNA replication by siRNA-mediated knockdown of CCT5 results in reduction of the propagation of the infectious virus.

Discussion

The chaperone-assisted protein-folding pathway is a process in living cells that results from coordinated interactions between multiple proteins that often form multi-component complexes. Several steps in the viral life cycle, such as protein processing, genome replication, and viral assembly, are regulated by cellular chaperones. Hsp90, one of the most abundant proteins in unstressed cells, has been implicated in HCV RNA replication (Nakagawa et al., 2007; Okamoto et al., 2006, 2008; Taguwa et al., 2008, 2009; Ujino et al., 2009). FKBP8, a member of the FKBP506-binding protein family, and hB-ind1, human butyrate-induced transcript 1, play key roles through their interaction with HCV NS5A and Hsp90 (Okamoto et al., 2006, 2008; Taguwa et al., 2008, 2009). Hsp90 has also been implicated in viral enzymatic activities including those of the influenza virus (Momose et al., 2002; Naito et al., 2007), herpes simplex virus (Burch and Weller, 2005), Flock house virus (Kampmueller and Miller, 2005), and hepatitis B virus (Hu et al., 2004).

In our former study, comparative proteome analyses of the viral RC-rich DRM fractions prepared from subgenomic replicon cells and Huh-7 cells were carried out to identify host factors involved

in HCV replication (Hara et al., 2009). We extended the proteomics by modifying our protocol of the analysis to reduce the interline differences in culture background and analyzed the DRM samples derived from the mid-log and confluent-growth phases of single cell line. Here, we identified two proteins, CCT5 and Hsc70, showing an increase in levels at the mid-log growth phase. Although CCT5 was also identified in the former study as expected, Hsc70 was not included in the list of proteins identified in the study (Hara et al., 2009). This difference may be due to the use of cells carrying the full-length replicon RNA in this study.

In this study, we demonstrated that TRiC/CCT participates in HCV RNA replication and virion production possibly through its interaction with NS5B. TRiC/CCT is a group II chaperonin that assists in protein folding in eukaryotic cells and forms a double-ring-like hexadecamer complex. Although relatively little is known about its function compared with that of the group I chaperonins such as bacterial GroEL, several mammalian proteins whose folding is mediated by TRiC/CCT have been identified, such as actin, tubulin, and von Hippel–Lindau tumor suppressor protein (Farr et al., 1997; Feldman et al., 2003; Frydman and Hartl, 1996; Meyer et al., 2003; Tian et al., 1995). With regard to viral proteins, the Epstein–Barr virus nuclear antigen, HBV capsid protein, and p4 of M-PMV have been identified as TRiC/CCT-interacting proteins (Yam et al., 2008). However, the functional significance of their interactions in the viral life cycles has yet to be determined. Here we demonstrated that the reduction in CCT5 expression in HCV replicon cells and in virus-infected cells inhibits HCV RNA replication (Figs. 3B and C) and virus production (Fig. 6) respectively. Gain-of-function was also shown by co-transfection of the replicon cells with eight constructs corresponding to all the TRiC/CCT subunits (Figs. 3A and D).

A recent study of the three-dimensional structure of the TRiC/CCT and Hsc70 complex has demonstrated that the apical domain of the CCT2 (CCT-beta) subunit is involved in the interaction with Hsc70 (Cuéllar et al., 2008). The complex formation created by the TRiC/CCT and Hsc70 interaction may promote higher efficiency in the folding of certain proteins (Cuéllar et al., 2008). In our comparative proteome analyses, both CCT subunits and Hsc70 were enriched in the HCV RC-rich membrane fraction of the replicon cells that showed high viral replication activity (Fig. 2B). Transfection of Hsc70 siRNA into the replicon cells moderately inhibited viral RNA replication (Fig. 3B). However, upregulation of HCV replication was not observed by ectopic expression of Hsc70 (Fig. 3A), and little or no interaction was observed between Hsc70 and HCV NS proteins in the co-immunoprecipitation analysis (data not shown). Thus, it is likely that TRiC/CCT acts as a regulator of HCV replication through participating in the de novo folding of NS5B RdRp, and Hsc70 might serve to assist in folding through its interaction with TRiC/CCT. It was recently reported that Hsc70 is associated with HCV particles and modulates the viral infectivity (Parent et al., 2009). Here we showed an additional role of Hsc70 in the HCV life cycle.

HCV genomic single-stranded RNA serves as a template for the synthesis of the full-length minus strand that is used for the overproduction of the virus-specific genomic RNA. NS5B RdRp is a single subunit catalytic component of the viral replication machinery responsible for both of these processes. It is known that the in vitro RdRp activity of recombinant NS5B expressed in and purified from insect cells and *Escherichia coli* is low in many cases. This could be due to the lack of a suitable cellular environment for favorable RdRp activity, although the particular conformational features dependent on the viral isolates may also be involved (Lohmann et al., 1997; Weng et al., 2009). In fact, besides interacting with HCV NS proteins, NS5B has been reported to interact with several host cell proteins. For example, human vesicle-associated membrane protein-associated protein subtype A (VAP-A) and subtype B (VAP-B), which are involved in the regulation of membrane trafficking, lipid transport and metabolism, and the unfolded protein response, interact with NS5B and NS5A and participate in HCV replication (Hamamoto et al., 2005). Recently, VAP-C, a splicing variant of VAP-B, was found to act as a negative regulator of viral replication through its interaction with NS5B but not with VAP-A (Kukihara et al., 2009). Cyclophilin A and B, peptidyl-prolyl isomerases that facilitate protein folding by catalyzing the *cis–trans* interconversion of peptide bonds at proline residues, play a role in stimulating HCV RNA synthesis through interaction with NS5B (Liu et al., 2009; Watashi et al., 2005). SNARE-like protein (Tu et al., 1999), eIF4AII (Kyono et al., 2002), protein kinase C-related kinase 2 (Kim et al., 2004), nucleolin (Kim et al., 2004; Hirano et al., 2003; Shimakami et al., 2006), and p68 (Goh et al., 2004) are also known to associate with NS5B and are possibly involved in HCV RNA replication.

We found that the aa 71–214 region in NS5B is important for interaction with TRiC/CCT. The catalytic domain of HCV RdRp has a "right-hand" configuration similar to other viral polymerases, such as HIV-1 reverse transcriptase (Huang et al., 1998) and poliovirus RdRp (Hansen et al., 1997), and is divided into the fingers, palm, and thumb functional subdomains (Lohmann et al., 2000). The region required for the interaction with TRiC/CCT has been mapped in a part of the fingers and palm domains of NS5B RdRp. To address how TRiC/CCT assists in the correct folding or disaggregation of NS5B through their interaction, leading to the formation of a functional RdRp, work based on an in vitro reconstitution system using purified proteins is under way. As all the TRiC/CCT subunits possess essentially identical ATPase domains, their protein-recognition regions are apparently divergent, allowing for substrate-binding specificity. It has recently been reported that TRiC/CCT interacts with the PB2 subunit of the influenza virus RNA polymerase complex and TRiC/CCT binding site is located in the central region of PB2, suggesting involvement of TRiC/CCT in the influenza virus life cycle (Fislová et al., 2010). Eukaryotic RNA polymerase subunit has also been identified as a binding partner of TRiC/CCT from interactome analysis (Yam et al., 2008). It would be interesting to examine how conserved the mechanisms of TRiC/CCT action that result in enhanced replication are among RNA polymerases.

The recruitment of a chaperonin by viral NS proteins may be important for understanding regulation of the viral genome replication. In this study, we demonstrated the involvement of TRiC/CCT in HCV RNA replication possibly through its interaction between TRiC/CCT and HCV NS5B. Although possible interaction of subunit CCT5 with NS5B was shown, considering involvement of whole TRiC/CCT complex in its chaperonin function, whether CCT5 directly interacts with NS5B is unclear. Further detailed studies are needed to make clear the manner of TRiC/CCT-NS5B interaction. NS5B RdRp is one of the main targets for HCV drug discovery. The search for NS5B inhibitors has resulted in the identification of several binding sites on NS5B, such as the domain adjacent to the active site and the allosteric GTP site (De Francesco and Migliaccio, 2005; Laporte et al., 2008). The findings obtained here suggest that disturbing the interaction between NS5B and TRiC/CCT may be a novel approach for an antiviral chemotherapeutic strategy.

Materials and methods

Cell culture, transfection, and infection

Human hepatoma Huh-7 and Huh-7.5.1 cells (kindly provided by Francis V. Chisari from The Scripps Research Institute) and human embryonic kidney 293T cells were maintained in Dulbecco's modified Eagle's medium (DMEM) supplemented with 10% fetal calf serum. Huh-7-derived SGR-N (Shi et al., 2003) and RCYM1 (Murakami et al., 2006) cells, which possess subgenomic replicon RNA from the HCV-N strain (Guo et al., 2001; Ikeda et al., 2002) and genome-length HCV RNA from the Con 1 strain (Pietschmann et al., 2002), were cultured in the above medium in the presence of 1 mg/ml G418. Cells were transfected with plasmid DNAs using FuGENE transfection reagents

(Roche Diagnostics, Tokyo, Japan). Culture media from Huh-7 cells transfected with in vitro-transcribed RNA corresponding to the full-length HCV RNA derived from the JFH-1 strain (Wakita et al., 2005) were collected, concentrated, and used for the infection assay (Aizaki et al., 2008).

Ab

Primary Abs used in this study were mouse monoclonal Abs against FLAG (Sigma-Aldrich, St. Louis, MO), c-myc (Sigma-Aldrich), CCT5 (Abnova Corporation, Taipei City, Taiwan), flotillin-1 (BD Biosciences, San Jose, CA), glyceraldehyde-3-phosphate dehydrogenase (GAPDH) (Chemicon, Temecula, CA), BrdU (Caltag, CA) and HCV NS5A (Austral Biologicals, San Ramon, CA), a rabbit polyclonal Ab against hemagglutinin (HA; Sigma-Aldrich), a sheep polyclonal Ab against bromodeoxyuridine (Biodesign International, Saco, ME), and goat polyclonal Abs against the individual subunits of CCT (Santa Cruz Biotechnology, Santa Cruz, CA) and Hsc70 (Santa Cruz Biotechnology). Anti Hsc70 and CCT5 monoclonal rat Abs were obtained from Abcam (Tokyo, Japan) and AbD serotec (Oxford, UK). Rabbit polyclonal antibody to NS5A was described previously (Hamamoto et al., 2005). Anti NS5B monoclonal Ab was kindly provided by D. Moradpour (Centre Hospitalier Universitaire Vaudois, University of Lausanne; Moradpour et al., 2002).

Plasmids

To generate expression plasmids for the NS proteins with dual epitope tags, DNA fragments encoding the NS3, NS5A, or NS5B proteins were amplified from HCV strain NIHJ1 (Aizaki et al., 1998) by PCR and cloned into the EcoRI–EcoRV sites of pcDNA3-MEF, which includes the MEF tag cassette containing the *myc* tag, TEV protease cleavage site, and FLAG tag sequences (Ichimura et al., 2005; Shirakura et al., 2007). To create a series of NS5B truncation mutants, each fragment was amplified by PCR and cloned into the EcoRI–XhoI site of pCMV-HA (Clontech, Mountain View, CA). To generate expression plasmids for the individual CCT subunits, cDNA fragments encoding human CCT1 through CCT8 were amplified from the total cellular RNA by RT-PCR and then cloned into the SmaI site of pCAGGS (Niwa et al., 1991). All PCR products were confirmed by nucleotide sequencing.

Proteome analysis

RC-rich membrane fractions from the cells were isolated as described previously (Aizaki et al., 2004). Briefly, cells were lysed in hypotonic buffer. After removing the nuclei, the supernatants were mixed with 70% sucrose, overlaid with 55% and 10% sucrose, and centrifuged at 38,000 rpm for 14 h. Proteins from the membrane fractions were then analyzed by 2D-DIGE as described previously (Hara et al., 2009). Briefly, protein samples were resolved in protein solubilization buffer (Bio-Rad Laboratories, Tokyo, Japan) and washed with pH adjustment buffer (7 M urea, 2 M thiourea, 4% CHAPS, 30 mM Tris–HCl [pH 10.0]), before being labeled with fluorescent dyes; the dyes used were Cy3 for RCYM1 cells samples taken at the exponential growth phase, Cy5 for cells samples taken at the confluent phase, and Cy2 for a protein standard containing equal amounts of both cell samples. Aliquots of the labeled samples were pooled and applied to Immobiline DryStrip (GE Healthcare, Tokyo, Japan) for first-dimension separation and to 12.5% polyacrylamide gels for second-dimension separation. Images of the 2-D gels were captured on a Typhoon scanner (GE Healthcare), and analyzed quantitatively using DeCyder v5.0 software (GE Healthcare). Samples were analyzed in triplicate as independent cultures and the Student's *t*-test was applied using the DeCyder biological variation analysis module to validate the significance of the differences in spot intensity detected between the samples.

In vitro RNA replication assay

In vitro replication of HCV RNA was performed as described previously (Hamamoto et al., 2005). Briefly, cytoplasmic fractions of subgenomic replicon cells were treated with 1% NP-40 at 4 °C for 1 h, followed by being incubated with 1 mM of ATP, GTP, and UTP; 10 μM CTP; [^{32}P]CTP (1 MBq; 15 TBq/mmol); 10 μg/ml actinomycin D; and 800 U/ml RNase inhibitor (Promega, Madison, WI) for 4 h at 30 °C. RNA was extracted from the total mixture by using TRI Reagent (Molecular Research Center, Cincinnati, OH). The RNA was precipitated, eluted in 10 μl of RNase-free water, and analyzed by 1% formaldehyde-agarose gel electrophoresis. For the immunodepletion assay, the cytoplasmic fractions were incubated with anti-CCT5 Ab in the presence of NP-40 for 4 h before NTP incorporation.

MALDI-TOF MS analysis

Target spots were cut and collected from gels under UV luminescence and rechecked with Typhoon scanner. The spot gels of the target proteins were subjected to in-gel trypsin digestion and analyzed by MALDI-TOF MS meter (Voyager-DE STR, Applied Biosystems, Tokyo, Japan) as described previously (Yanagida et al., 2000). All proteins were identified by peptide mass fingerprinting.

Immunoblot analysis and immunoprecipitation

Immunoblot analysis was performed essentially as described previously (Aizaki et al., 2004). The membrane was visualized with SuperSignal West Pico chemiluminescent substrate (Pierce, Rockford, IL). For immunoprecipitation, cells transfected with plasmids expressing epitope-tagged HCV protein or CCT5 were lysed and then subjected to two-step precipitations with anti-myc and anti-FLAG Abs according to the procedures described previously (Ichimura et al., 2005). In some experiments, HA-tagged full-length NS5B (aa 1–591) or its deletion mutants (aa 71–591, 215–591, 320–591, 1–570) were co-expressed with CCT5 in cells, followed by single-step immunoprecipitation and immunoblotting.

Immunofluorescence staining

Cell permeabilization with lysolecithin and detection of de novo-synthesized viral RNA was performed as described previously (Shi et al., 2003). Briefly, Huh-7 cells were plated on 8-well chamber slides at a density of 5×10^4 cells per well. Cells were incubated with actinomycin D (5 μg/μl) for 1 h and were washed twice with serum-free medium, before being incubated for 10 min on ice. The cells were then incubated in a transcription buffer containing 0.5 mM BrUTP for 30 min. The cells were fixed in 4% formaldehyde for 20 min and then incubated for 15 min in 0.1% Triton X-100 in phosphate-buffered saline (PBS). Primary Abs were diluted in 5% bovine serum albumin in PBS and were incubated with the cells for 1 h. After washing with PBS, fluorescein-conjugated secondary Abs (Jackson Immunoresearch Laboratories, West Grove, PA) were added to the cells at a 1:200 dilution for 1 h. The slides were then washed with PBS and mounted in ProLong Antifade (Molecular Probes, Eugene, OR). Confocal microscopy was performed on a Zeiss Confocal Laser Scanning Microscope LSM 510 (Carl Zeiss MicroImaging, Thornwood, NY).

RNA interference

Small interfering RNAs (siRNAs) targeted to CCT5 or Hsc70 and scrambled negative control siRNAs were purchased from Sigma-Aldrich Japan (Tokyo, Japan). Cells were plated on a 24-well plate with